Tracking Cytotoxic T-cell degranulation in diverse cholesterol conditions

A Thesis

submitted to

Indian Institute of Science Education and Research Pune in partial fulfilment of the requirements for the BS-MS Dual Degree Programme

by

Amogh Vinay Ranade

Indian Institute of Science Education and Research Pune

Dr. Homi Bhabha Road,

Pashan, Pune 411008, INDIA.

Date: 15th March, 2024

Under the guidance of

Supervisor: Dr Sudha Kumari,

Indian Institute of Science

From May 2023 to March 2024

INDIAN INSTITUTE OF SCIENCE EDUCATION AND RESEARCH PUNE

Certificate

This is to certify that this dissertation entitled **Tracking cytotoxic T-cell degranulation in diverse cholesterol conditions** towards the partial fulfilment of the BS-MS dual degree programme at the Indian Institute of Science Education and Research, Pune, represents study/work carried out by Amogh Vinay Ranade at the Indian Institute of Science under the supervision of Dr. Sudha Kumari, Assistant Professor, Department of Microbiology and Cell Biology, during the academic year 2023-2024.

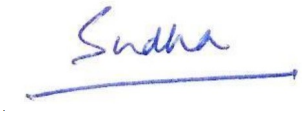

Amogh Vinay Ranade
Roll No. 20191009

Dr. Sudha Kumari
Assistant Professor
Indian Institute of Science

Committee:
Supervisor: Dr. Sudha Kumari
TAC Member: Dr. Satyajit Rath

This thesis is dedicated to both my parents and sister. Thank you for your love and constant support. You have always inspired me with your strength, resilience, and passion for learning.

Declaration

I hereby declare that the matter embodied in the report entitled **Tracking cytotoxic T-cell degranulation in diverse cholesterol conditions** are the results of the work carried out by me at the Department of Microbiology and Cell Biology, Indian Institute of Science, Bengaluru, under the supervision of Dr. Sudha Kumari, and the same has not been submitted elsewhere for any other degree. Wherever others contribute, every effort is made to indicate this clearly, with due reference to the literature and acknowledgement of collaborative research and discussions.

Amogh Vinay Ranade

Roll no. 20191009

Date: 15th March 2024

Contents

List of Figures

Abbreviations

APC	Antigen Presenting Cell
CD	Cluster of Differentiation
cSMAC	central Supramolecular Activation Complex
CTL	Cytotoxic T Lymphocyte
dSMAC	distal Supramolecular Activation Complex
GEF	Guanine nucleotide Exchange Factor
HSC	Haemopoietic Stem Cells
ICAM1	Intercellular Adhesion Molecule 1
IP3	Inositol Trisphosphate
LAT	Linker for Activation of T-cells
LFA	Lymphocyte Function-associated Antigen
MβCD	Methyl-β-cyclodextrin
MHC	Major Histocompatibility Complex
MPP	Multipotent Progenitors
MTOC	Microtubule organizing center
NFAT	Nuclear Factor of Activated T-cells
NF-κB	Nuclear Factor-κB
NK	Natural Killer
NPF	Nucleation Promoting Factor
PBS	Phosphate Buffer Saline
PKC	Protein Kinase C
PLCγ	Phospholipase C gamma
PMA	Phorbol Myristate Acetate
pMHC	peptide Major Histocompatibility Complex
pSMAC	peripheral Supramolecular Activation Complex
PTK	Protein Tyrosine Kinases
RAC	Ras related C3 botulinum toxin substrate 1
RCF	Relative Centrifugal Force
RPM	Revolutions per minute
RPMI	Rosewell Park Memorial Institute
SLP76	SH2 domain containing Leucocyte Protein of 76kDa
SMAC	Supramolecular Activation Complex
SRC	Short for ‘Sarcoma’
SYK	Spleen Tyrosine Kinase
TCR	T-Cell Receptor
TEC	Tyrosine Protein Kinase
U-Drug	U18666A
ZAP 70	Zeta-chain-associated protein kinase 70

Abstract

Adaptive immunity is vital for surveillance and protection against internal and external threats. It is also essential for pathogen clearance and maintaining immune homeostasis in organisms. CD8+ cytotoxic T-cells (CTLs) are central players in adaptive immunity. They can kill infected/cancerous cells by forming specific and directional immunological synapses with them and releasing cytotoxic granules at the synaptic interface. Although this has been established in previous studies, the precise molecular machinery involved in the delivery and the release of the granules at the synapse remains unclear. Additionally, cholesterol seemingly plays a critical role in CTL activation and effector response, but its functional pathways are yet to be brought to light. We address both these questions by modulating the membrane cholesterol levels of CTLs with the help of pharmacological inhibitors such as MβCD and U-Drug and look at the extent of degranulation in response to these treatments under various activation conditions. This analysis reveals that while the aforementioned drugs demonstrably influence the intracellular movement of granules, they don't significantly impact the degranulation process. This implies that the two processes are decoupled to a large extent and thus can be regulated independently.

Acknowledgements

As they say, all good things must come to an end, and thus, as my time at the immunosurveillance lab draws to a close, I would like to take this opportunity to thank everyone who helped me during my time in Bengaluru. I am grateful to all of you.

I would like to express my sincere gratitude to my thesis supervisor, Dr. Sudha Kumari, for giving me the opportunity to pursue my MS thesis at her lab in IISc. Your mentorship, guidance, and support really helped me learn and grow. You always gave me enough space to make my own mistakes and provided input whenever I needed it. Thank you for that. A big thank you to my lab mates, Srishti, Sayanti, Maha, Sikha, Aheria, Priyobrata, Aditya, Rishab, Diptanshu, Mahitha and Sandeep. It was great fun going out for coffee with you guys after lab meets. Thank you for always tolerating my “small clarifications” and patiently explaining concepts to me, and thank you for teaching me so many new techniques. I heartfully thank the Department of Microbiology and Cell Biology at IISc for providing me with the facilities to complete my master's thesis.

As the completion of this thesis brings my time at IISER Pune to an end as well, I would like to thank all my friends who made my time at IISER memorable. There are too many names to name, but I am grateful to each and every one of you for making my college years memorable. I want to thank my family for their unwavering love and support and for always being inquisitive about the work that I was doing, irrespective of whether you understood it completely or not.

And to anyone who has ever asked me about my work or shown an interest in what I do, thank you for your curiosity and enthusiasm. This thesis reflects the love and support of so many exceptional individuals; I am genuinely grateful.

Contributions

Contributor name	Contributor role
Amogh Ranade, Dr. Sudha Kumari	Conceptualization Ideas
Amogh Ranade, Dr. Sudha Kumari	Methodology
-	Software
Amogh Ranade	Validation
Amogh Ranade	Formal analysis
Amogh Ranade, Dr. Sudha Kumari	Investigation
Sudha Kumari	Resources
Amogh Ranade, Dr. Sudha Kumari	Data Curation
Amogh Ranade	Writing - original draft preparation
Dr. Sudha Kumari	Writing - review and editing
Amogh Ranade, Dr. Sudha Kumari	Visualization
Dr. Sudha Kumari	Supervision
Dr. Sudha Kumari	Project administration
Dr. Sudha Kumari	Funding acquisition

This contributor syntax is based on the Journal of Cell Science CRediT Taxonomy[1].

[1] https://journals.biologists.com/jcs/pages/author-contributions

Introduction

Immunity, from its Latin word *immunis*, is the state of being insusceptible or resistant to a noxious agent or process, and Immunisation is the production of immunity in an organism (*Immunity, Immunization - Quick search results | Oxford English Dictionary*). People have been employing the principles of immunization without fully understanding the concepts of immunity in multiple regions of the world for many years. Wan Quan's account of smallpox variolation in 1549 was one of the first documented instances of immunization in China (Needham, 2000). Many years later, this method was reintroduced by English physician Edward Jenner to target smallpox again using cowpox pustule fluid (Riedel, 2005). There have also been Egyptian reports from the Ebers Papyrus describing how Imhotep externally infected tumours using a poultice to induce their regression and partially ease patient distress (Radha and Lopus, 2021). This concept was brought back by William Coley, who used heat-killed Streptococcus as a vaccine against sarcomas (McCarthy, 2006). Taking note of these instances, it's safe to say that we have come a long way in terms of the knowledge that we now have about the functioning and the mechanistic underpinnings of immunity.

The vertebrate immune system represents an essential organ system indispensable for the survival of multicellular organisms. Its primary function is maintaining a healthy homeostatic state through a coordinated response against pathogenic entities. This multifaceted response can be demarcated into three major functions. First is the direct elimination of these entities and other atypical cells within the organism. Secondly, the generation of specific, potent and long-lasting immunological memory during this process of elimination, and thirdly, maintaining a fine balance to optimise pathogen clearance while minimising collateral damage due to healthy host cells getting caught in the crossfire.

Mammalian immunity has at least two components that mediate function- the cellular and the humoral. Cellular immunity consists of all the immune cells that provide protection against both intracellular and extracellular pathogens in a direct manner, such as through phagocytosis or by triggering apoptosis. Alternatively, humoral immunity comprises innate and adaptive soluble factors like antibodies (Charles A Janeway et al., 2001a). Throughout my thesis, I will focus on one of the central cell types contributing to cell-mediated immunity, the T Lymphocytes (Broere and van Eden, 2019).

T Lymphocytes belong to a much broader blood cell type called the leucocytes (White Blood Cells), all arising from the Haemopoietic stem cells (HSC). HSCs give rise to Multipotent Progenitors (MPP), which in turn give rise to granulocytes, antigen-presenting cells (APC) and lymphocytes. The granulocytes comprise of neutrophils, eosinophils, basophils, and mast cells which are primary components of innate immunity. Similarly, monocytes, macrophages and dendritic cells contribute to the APC pool. APCs process and display an array of neo-antigens from the pathogen as small peptide sequences through MHC class I or class II molecules for other adaptive immune cells to recognise and to act on. Lymphocytes are found in peripheral tissue spaces and constantly circulate through the lymphatic and circulatory systems. They drain into the lymph nodes, where oftentimes they encounter APCs. Lymphocytes are further divided into subtypes based on proteins that they express on the cell surfaces called Cluster Differentiation (CD) proteins. Some major classes of Lymphocytes are the B cells, the T cells and the NK cells. These classes are further subdivided based on more specific cell surface markers. A brief schematic outlining the cell types and their developmental origins and trajectories has been shown in Figure 1.

Another distinct classification method involves the developmental lineage, functional parameters and time of action after infection of immune cells. This method of classification differentiates between innate and adaptive immunity. The term ‘Innate’, which has been borrowed from Latin, loosely translates to ‘existing at the time of birth’ and thus, Innate immunity is an umbrella term for all the immune cell types that organisms are born with (Charles A Janeway et al., 2001b). Due to this, the innate immune system forms the first line of defence. The nature of the threats the innate immune system deals with are quite diverse and sudden; thus, its cells are fast-acting but non-specific (Vivier and Malissen, 2005). Complimentarily, the adaptive immune system is relatively slower-acting and highly specific (Vivier and Malissen, 2005). It completely develops in humans around 2 years of age. It shows a very large diversity both in its cell types and individual cell heterogeneity within a cell type (Vivier and Malissen, 2005). These mechanisms are in place to aid its adaptability and to fight against a plethora of pathogens. It also has some additional characteristics where it can generate long-lasting memory and has a persistent and highly regulated effector response. T and B lymphocytes are categorized under the adaptive immune system. In terms of order of action, typically, the innate immune system tries to fight the infection first, and if it cannot, adaptive immunity kicks in (Charles A Janeway et al., 2001b).

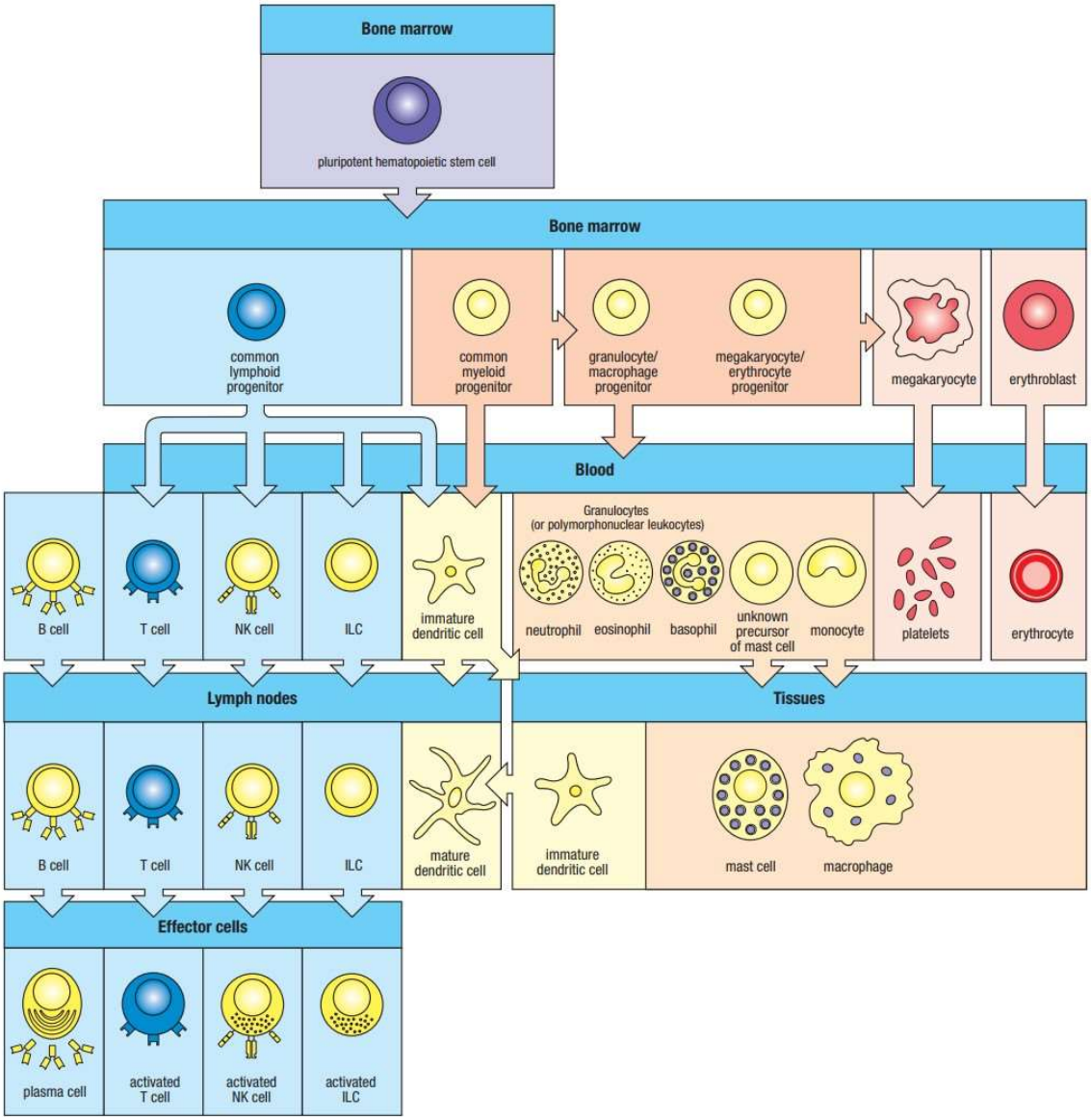

Figure 1- Schematic of the origin of the different immune cell types (Charles A Janeway et al., 2001c)

One of the primary functions of the immune system is to carry out surveillance in the body (Ribatti, 2016). This surveillance like any other is done by inspecting and differentiating self/non-self in an error free yet time efficient manner. The immune system receives a barrage of signals through numerous pathways. It can detect digested peptides or foreign DNA from pathogens, it can detect chemicals such as cytokines released by other immune cells which in many cases point to loss in immune homeostasis. What's worthwhile to note is that the responses to these external cues are graded and dynamic.

Immune cells employ 3 different cytotoxicity pathways to get rid of disease-causing cells which are, direct contact, indirect contact and chemical stimulation (LI et al., 2015). Chemically stimulated cytotoxicity is where cells undergo apoptosis due to cues present in the extracellular environment. These cues are secreted by other immune cells that are not necessarily in close proximity to the cells that they act on. This cytotoxicity is non-specific and acts in a widespread manner. Direct contact cytotoxicity, on the other hand, is a characteristic feature of T-cells and NK cells and is highly specific (Minute et al., 2020). In T lymphocytes, especially CD8+ T-cells, cytotoxicity can be mediated through Fas-FasL interaction and the pMHC-TCR interaction (Charles A Janeway et al., 2001d). The Fas-FasL interaction is a self-regulatory mechanism established to eliminate potentially harmful T-cells (Shrestha and Diamond, 2007). Conversely, pMHC-TCR interaction triggers direct contact cytotoxicity-mediated killing (Charles A Janeway et al., 2001d). This pMHC-TCR interaction that takes place between the CD8+ T-cell and the target cell is the central pathway that effector CD8+ T-cells use for killing. Mechanistically, depending on the strength of the pMHC-TCR interaction, a downstream cascade of signalling can be triggered, eventually resulting in the directional degranulation of CD8+ T-cells (Ma et al., 2012).

Degranulation is not limited to effector T lymphocytes. It's a much more widespread phenomenon exhibited by many immune cell types where they release certain specialized antimicrobial compounds which are stored in membrane bound vesicles called cytotoxic granules, in response to stimuli (Mok et al., 2021). It's an essential immune response exhibited by Lymphocytes, macrophages, neutrophils, mast cells, eosinophils, and basophils (Mok et al., 2021). Depending on the substances released, this process can regulate inflammation and carry out directed cell killing. Dysregulation of degranulation can lead to various immune disorders and diseases, such as autoimmune diseases and cancer. The two major cell types that carry out directed cell mediated killing through degranulation across an immune synaptic interface are NK cells and T-cells (Charles A Janeway et al., 2001d; Dustin and Long, 2010; Prager and Watzl, 2019). Now, focussing on CD8+ T-cell degranulation again, there are multiple stages between the first pMHC-TCR interaction and the final step of degranulation. They are briefly described below.

Firstly, Cytotoxic T cells recognize their target cells through the interaction between their TCR and the peptide-MHC complex displayed on the target cell's surface. Numerous such peptide-MHC and TCR interactions lead to the formation of the immunological synapse, a specialized contact region with a relatively conserved arrangement of molecules at the plane of the interface of the two cells (Dustin, 2014, p. 20). Once a stable immunological synapse is formed, T-cells undergo a series of immediate downstream phosphorylations, which ultimately increase the cytoplasmic calcium concentration of T-cells (Angus and Griffiths, 2013). After stabilising the immunological synapse, the CTL polarizes its microtubule-organizing centre (MTOC) towards the synapse.

The MTOC reorganisation leads to the reorientation of granules and promotes their directional transport towards the immune synapse. The granules then dock near the immunological synapse awaiting degranulation. It's important to note that all these steps happen initially during the priming of the CTLs with specific antigens. This priming generally happens in the lymph nodes through APCs. It's the first round of activation which triggers the production of granules in the CTLs. These cells do not degranulate immediately after this activation. Instead, they produce and sequester the granules within them so that they can degranulate thereafter. These primed CTLs are sent out into circulation again where they carry out immunosurveillance. Upon encountering a specific antigen again such that the threshold for pMHC-TCR signalling is crossed, the cytotoxic T cell releases the contents of its granules onto the target cell. The major components of cytotoxic granules are Perforin, Granzyme B and Granulysin (Charles A Janeway et al., 2001d). Perforin perforates the cell membrane of the target cell (Osińska et al., 2014). Granzyme B which is the most powerful pro-apoptotic member of the Granzyme family, has a caspase-like activity to cleave substrates. It can also cleave and activate many procaspases directly (Trapani, 2001). In these ways it triggers the apoptosis pathway, thereby killing and exposing any intracellular pathogens that might be residing within the target cell (Sutton et al., 2000). Granulysin is a unique cytolytic pro-inflammatory molecule only found in humans (Krensky and Clayberger, 2009). Along with perforin, it eliminates the intracellular pathogens (Hanson et al., 1999). Granulysin also independently has antimicrobial activity where it can directly kill bacteria, fungi and parasites. It does so by entering the target cells and perforating the cell walls of the intracellular pathogens (Stenger et al., 1998). The cytotoxic granules also contain anchor proteins such as serglycin which are responsible for effective storage and protection of the antimicrobials inside the granules (Korpetinou et al., 2014).

CTL Degranulation at the immunological synapse thus plays an essential role in adaptive immunity (Cassioli and Baldari, 2022). It can potentially control the efficiency and the specificity of the response mounted against various infections as well as cancer, and thus, it is a central area of study. Altering the extent of degranulation could potentially be used to tune CTL activity to regulate immune responses.

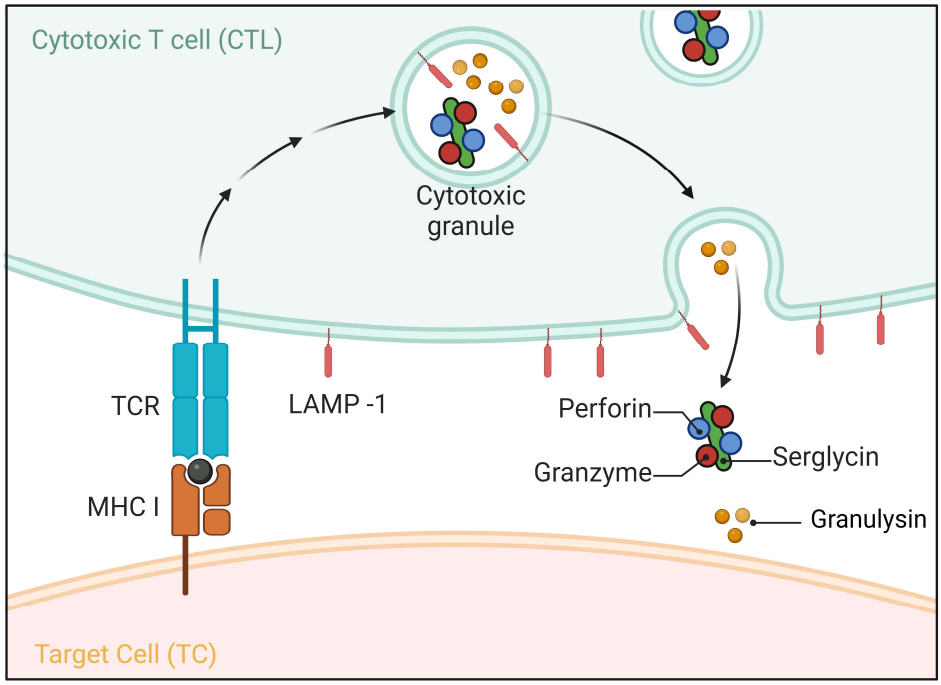

Figure 2 -- Schematic depicting degranulation in CTLs (Biorender.com)

Literature Review

The Immune Synapse

"Immunological synapses are antigen-specific cell-cell junctions with a synaptic cleft stabilized *by bona fide* adhesion molecules for vectorial cell-cell communication between an immune cell and an antigen-presenting cell" (Dustin, 2014). This definition of the immune synapse is succinct but it's worthwhile to break it down and elaborate on parts of it in a piecewise manner. The first phrase to focus on is 'antigen-specific'. Antigen specificity is an inherent property of the immunological synapse (Huppa and Davis, 2003). A relatively strong pMHC-TCR interaction is required to form the immunological synapse. Even though studies have shown that a single pMHC-TCR interaction is sufficient to trigger T-cell response (Huang et al., 2013), in most cases, a threshold number of pMHC-TCR interactions must be crossed to activate CTLs and trigger degranulation. The next part that should be focussed on is 'bona fide adhesion molecules.' This implies that there are specialized adhesion molecules that are present on the T-cell and the APC, such as LFA-1 and ICAM-1 which play a role in stabilizing the immune synapse (Dustin and Cooper, 2000). Finally, we need to appreciate 'vectorial' communication. In this case, it implies directional information transfer between the two cells. Molecules don't just travel by random diffusion in the synaptic cleft. There are mechanisms in place that help in the targeted delivery of cellular cargo. Another important thing worth pointing out is that there is bi-directional cargo transport. There has been evidence such as endocytosis of pMHC-TCR complexes and vesicular trafficking of other molecules into the T-cell (Liu et al., 2009) showing transport from the target cell to the T-cell. There has also been evidence of mitochondrial transfer from cancer cells to T-cells (Zhang et al., 2023).

Now that a basic understanding of the immune synapse has been established let's look at the spatial organisation of the immune synapse and the rationale behind its conserved structure. In 1998, Collin Monks and his team discovered that molecules participating in a typical CTL immune synapse, contrary to a homogenized distribution that you'd expect, are segregated into concentric regions which he termed as supramolecular activation clusters (SMACs) (Monks et al., 1998). Less than a year later it was shown that there is a surge of Intercellular Adhesion Molecule 1 (ICAM1) at the contact site between the 2 cells and TCR ligands were being transported to the cSMAC (Grakoui et al., 1999).

As the synapse progressed, ICAMs were pushed to the pSMAC and centre of the immune synapse was populated with TCR-MHC complexes. Since then, the organisation of the immune synapse has been extensively studied and many more molecular interactions have been characterized. Figure 4 shows a simplistic depiction of immune synapse based on our recent understanding of it.

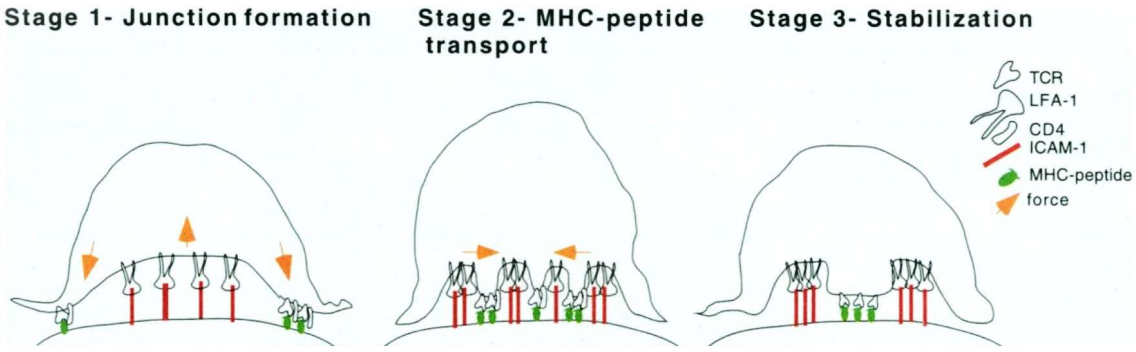

Figure 3- Model of formation of the Immunological synapse (Grakoui et al., 1999). Junction formation: T cell recognizes pMHC through TCRs and stop exploring further. MHC peptide transport: Transport of pMHC-TCR to the cluster centre mediated by actin. Stabilization: MHC's are "locked in" for effective signal transduction and activation.

Figure 4- Model Immunological synapse (Dustin, 2014). Black = F-actin lamellipodium, Blue = LFA1-ICAM1 adhesion, Red = TCR-MHC, Green = CD28-CD80 costimulatory molecules.

Having looked at the structural organisation of the immune synapse, it's important to briefly discuss downstream signal transduction in the T-cell following the formation of the immune synapse. There have been numerous studies recording the activities of protein regulators in T cell activation (Koretzky and Myung, 2001). The TCR by itself doesn't have tyrosine kinase activity. It compensates for that with cytosolic protein tyrosine kinases (PTKs) such as the SRC, SYK, and TEC families (Shah et al., 2021). These PTKs phosphorylate tyrosine residues within immunoreceptor tyrosine-based activation motifs (ITAMs) of various CD3 subunits, which forms the binding site for ZAP70, a SYK-family PTK. ZAP70 then subsequently phosphorylates LAT and SLP76, further relaying the signal (Finco et al., 1998; Yablonski et al., 1998; Żal et al., 2002). Activation of PLCγ1 by SLP76 leads to IP_3 production, which causes cytosolic free calcium accumulation. The phosphorylated SLP76 binds to VAV, which activates RAC/RHO GTPase activity that is essential for actin reorganization through the Guanine Nucleotide Factor (GEF) (Kraynov et al., 2000).

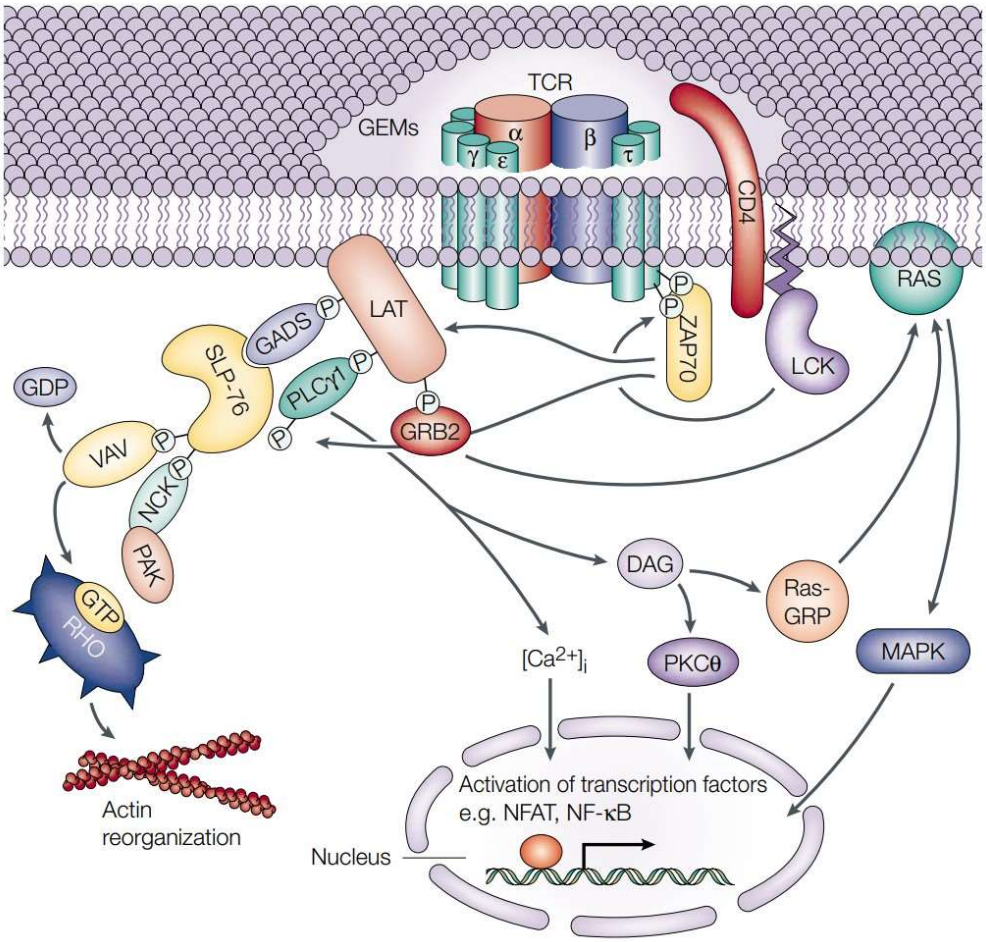

Figure 5- Downstream signal transduction in T-cells (Koretzky and Myung, 2001).

Cholesterol

There are various external factors that regulate CTL degranulation and the subsequent adaptive immune response. One such factor that has been studied previously to a large extent is the effect of cholesterol on effector T-cell activity. Cholesterol is an irreplaceable yet enigmatic molecule which plays significant roles in cellular function and maintaining homeostasis (Yeagle, 2022). It is ubiquitously found in cellular organelles and forms major parts of the endomembrane system where it fulfils multiple roles (Lippincott-Schwartz and Phair, 2010). Specifically, cholesterol plays a central role in T-cell function and thus perturbations made to cholesterol concentrations can have a major impact on their effector responses.

There have been quite a few studies investigating how altering cholesterol concentrations can lead to changes in CD4 and CD8 T-cell responses but the observations and the conclusions drawn from them have been varied and a unified mechanism of how cholesterol operates in facilitating/impeding T-cell function is absent (Heiniger et al., 1978; Ma et al., 2019; Yan et al., 2023; W. Yang et al., 2016). I will try to highlight some of the caveats and shortcomings of these studies due to which a consistent set of observations aren't available and a general causative mechanism cannot be proposed. The first caveat is the indispensability of cholesterol (Yeagle, 2022). Due to its essentiality in cell survival and cell health, perturbations to its concentrations within the cell are limited to ones that don't significantly hamper cell viability. Thus, a stark contrast can't be obtained to appreciate the differences in cell function perspicuously. The second point is the ubiquitous presence of cholesterol in most regions of the cell (S.-T. Yang et al., 2016). This is in part due to its indispensability but it poses a unique problem. The concentrations of cholesterol in the cell are very dynamic and never uniform (Ikonen, 2008). Cholesterol is in a constant state of flux where there are multi-step internal pathways that are responsible for cholesterol synthesis such as the mevalonate pathway and influx/efflux pumps found conserved in most cell types which are responsible for the uptake of dietary cholesterol and releasing cellular cholesterol into the blood stream. Thus, the cholesterol content of the cell is controlled by the uptake, biosynthesis and efflux all driven by intracellular sensors in a tight regulatory circuit (Hu et al., 2023). With so many potential points of intervention, regulating whole cell cholesterol levels is not pharmacologically feasible as one would have to use multiple drugs to target each of these pathways for cholesterol modulation. Not to mention that this could also compromise cell health.

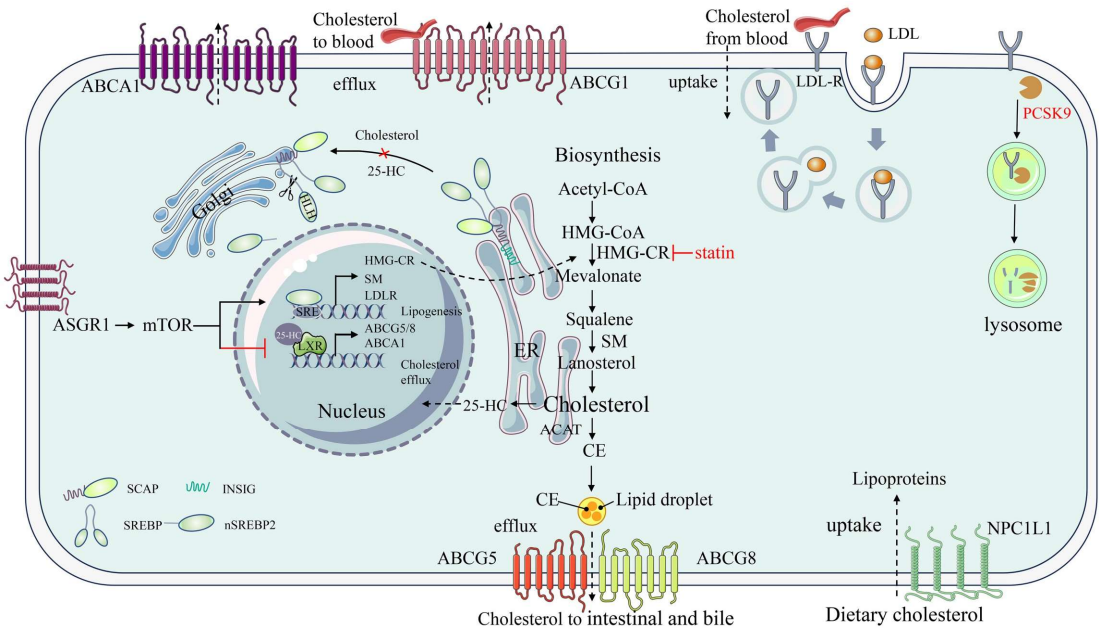

Figure 6- Cholesterol metabolism and mechanisms to maintain cholesterol homeostasis. (Hu et al., 2023)

Studies so far use pharmacological modulators that alter cholesterol levels for specific organelles. This is a great way of approaching the larger question where you compartmentalize and focus on specific regions of the cell. The problem that arises with this is that if the mechanistic understanding for the drug's action on cholesterol function in that subcellular region is not established then it's difficult to pinpoint why the altered phenotype is seen. What adds to this difficulty of cholesterol perturbation is that it doesn't have a universally stimulatory or inhibitory effect in terms of the effector phenotype readout. To elaborate on this, I will highlight two studies. Xingzhe Ma and colleagues showed how excessive cholesterol in the tumor microenvironment causes ER stress in the CD8+ Effector T-cells and the stress can be alleviated by depleting cholesterol (Ma et al., 2019). On the other hand, a study published by Chengsong Yan and colleagues underscored the fact that tumor infiltrating CD8+ effector T-cells were infact cholesterol deficient due to which they were not able to carry out effective tumor clearance (Yan et al., 2023). Both these studies have looked at cholesterol content in different pathways and that seems to be the primary reason why they have contradicting conclusions. Thus, depending on the subcellular compartment that the drug targets, you can have both activating and inhibitory effects.

Now that enough groundwork has been laid down to appreciate the complexity and nuances of the problem at hand, a transition can be made into the background of the specifics of the system that we used for the work done during my thesis. Previously in the lab, granular recruitment at the synapse has been studied through lattice light sheet microscopy. A planar lipid bilayer system was used for this, where the glass surface was coated with ICAM-1 and specific pMHC complexes which were conjugates for TCRs that the T-cells were expressing. These ligands were embedded in the bilayer to mimic the APC surface. The T-cells were treated with an array of pharmacological inhibitors and then were put onto the bilayer to form synapses. The imaging of these synapses was done and granular movement was characterized through different parameters such as distance, linear velocity, angular velocity and so on. Two of these small molecule inhibitors caused a discernible change in granule movement- Methyl-β-cyclodextrin (MβCD) and CK666. MβCD treatment slowed down granule movement in the cell implying that reduction in the cholesterol levels reduced the linear velocity and increased the distance of granular movement since it's a small molecule inhibitor that lowers the cholesterol in membranes of the cell. CK666 which is a small molecule actin polymerization inhibitor also had the same effect on granule movement where it showed reduced linear velocity. CK666 binds to the 7 subunit Arp2/3 complex which is an actin nucleating factor (ANF) (Hetrick et al., 2013). Arp 2/3 is responsible for branched chain actin formation where it acts as a hinge at the intersection of two F-actin strands (Mullins et al., 1998; Rotty et al., 2013). This implied that reduced branched chain actin formation caused a reduction in granule movement. This was hypothesized to be due to the fact that branched networked actin structures are necessary for facilitated diffusion across large areas (Rizvi et al., 2009). The data for this has been shown in figure 6.

Of these two, the effect of cholesterol reduction on granule movement was something we decided to pursue further as it had previously become apparent that the effect of cholesterol in T-cell effector function was unclear. To work around the generality and complexity of the question, we decided to study a specific case where we, characterized CTL degranulation while varying the cell membrane cholesterol content. Here we were restricting ourselves to the cell membrane which was optimal since it forms the interface where degranulation eventually takes place. It seemed like the natural next step after finding a reduction in granular movement after MβCD treatment. Thus, we have looked at the effect of cholesterol enriched/depleted cell membranes on degranulation efficiency in primed CTLs.

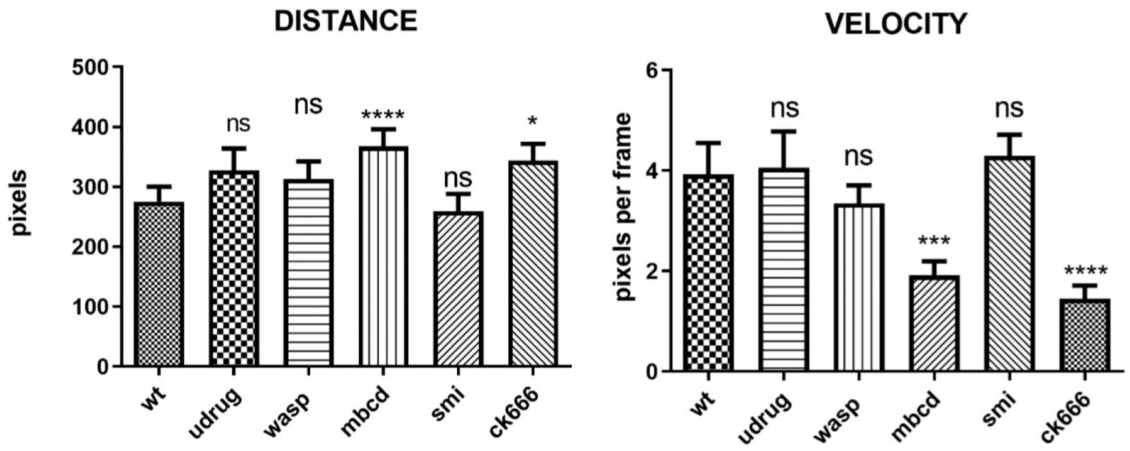

Figure 7 -Distance and velocity measurements of granular movement inside T-cells after treating with multiple small molecule inhibitors.

Cholesterol plays a consequential role in membrane dynamics, both in the cell membrane and the endomembrane system. It contributes to the membrane fluidity, thickness, compressibility and the intrinsic curvature of the membranes in which it resides (S.-T. Yang et al., 2016). Cholesterol plays an eminent role in TCR activation and clustering as well. It binds to the TCRβ chain of inactive receptors and maintains them in that state in the absence of stimulation and thus is an allosteric inhibitor of TCRs (Hu et al., 2023). Surprisingly though, an excess of cholesterol in the membrane can lead to enhanced TCR clustering which increases the avidity of the cell and lowers the threshold activation required by antigen stimulation (Pathan-Chhatbar et al., 2021). These are cardinal events that precede the formation of the immune synapse and can potentially affect degranulation.

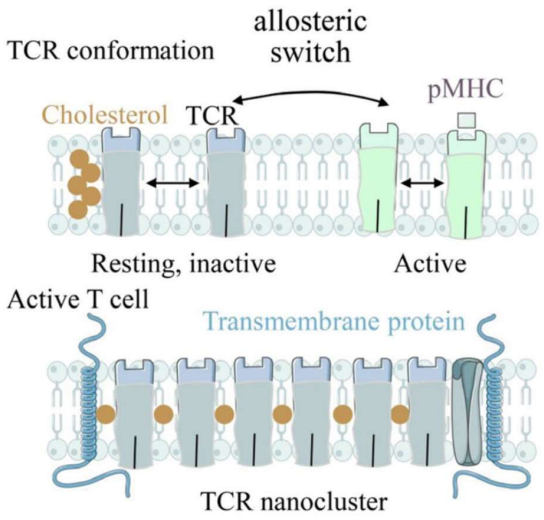

Figure 8- Arrangement of cholesterol in TCR conformations and clustering. (Hu et al., 2023)

Having touched upon cholesterol's role in T-cell activation, it's important to understand the role of the two small molecule inhibitors that we employed in order to enrich/deplete cholesterol in the cell membrane. They were Methyl-β-cyclodextrin (MβCD) and U18666A (U-Drug) respectively. Both of them have antagonistic effects on cell membrane cholesterol levels (Cenedella, 2009; van Gestel et al., 2005). MβCD is a cyclic oligosaccharide with α-1,4 glycosidic bonds. It is a widely used membrane cholesterol inhibitor (Ulloth et al., 2007). It's mechanism of action for cholesterol exclusion from the cell membrane is that it traps cholesterol within its cavity and in doing so disrupts the structure of lipid rafts as well (Mahammad and Parmryd, 2015; Rodal et al., 1999). It competitively excludes cholesterol in an irreversible manner and hence cells are very sensitive to the action of MβCD. It is generally used in low concentrations over very short time-scales in order to maintain cell viability. U-Drug on the other hand does the opposite of this and enriches the cell membrane and the endomembrane system with cholesterol by stagnating cholesterol transport (Song, 2022). U-Drug goes and binds to the sterol sensing site of Neimann-Pick C1 (NPC1) which is a lysosomal membrane protein (Lu et al., 2015). It is a cationic amphiphilic drug that accumulates in the acidic intracellular compartments of lysosomes (Salata et al., 2017). In doing so, it inhibits lysosomal cholesterol recycling and thus eventually cholesterol ends up accumulating in the cell membrane. It is not as toxic as MβCD and thus can be used at relatively higher concentrations and treatments are given for longer periods of time to obtain the desired effect. At these higher concentrations U-Drug stagnates cholesterol transport in the endoplasmic reticulum, golgi and cell membrane (Poh et al., 2012).

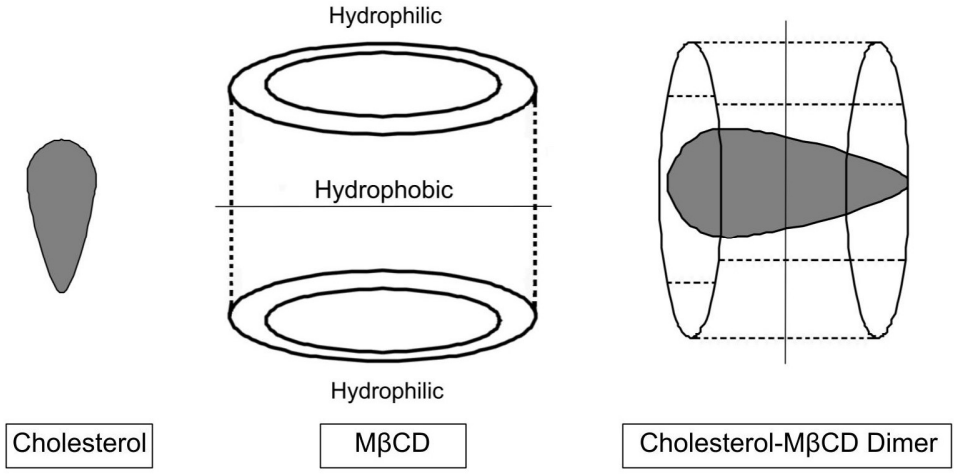

Figure 9 -Representative structures of Cholesterol, MβCD and their dimer (Mahammad and Parmryd, 2015)

Through this study, I aim to decipher the role of cell membrane cholesterol in the degranulation of cytotoxic T-cells and hope to provide functional insights into how cell membrane dynamics play a role in T-cell mediated cytotoxicity. Our findings could potentially provide targets for therapies to modulate T-cell cytotoxicity and thus heighten/dampen the adaptive immune response based on disease conditions.

Materials and Methods

Isolation of Immune cells from Mouse Lymph nodes and Spleen

A T25 Flask was coated with IgG antibody (100µg/ml). Mice were rendered unconscious using Isoflurane and then euthanized by cervical dislocation. The skin and fur were cut off over the mouse's ventral side (abdomen), taking care not to rupture the peritoneum. Inguinal (Lower side) and brachial (Upper side) lymph nodes were extracted by surgical forceps. They were muddled through a 40-micron cell strainer with the base of a sterile syringe piston. The mesenteric (middle) lymph node was extracted from the base of the intestine after cutting open the peritoneum. The spleen was extracted similarly, and both were passed through the 40-micron filter with the help of the base of a sterile syringe piston as well. The filtered cell suspension was centrifuged at 600rcf for 5 minutes at 4°C. To remove the RBC fraction, we added 1-2 ml of RBC lysis buffer (1X) and let it sit on ice for 7 minutes. The reaction was quenched with excess PBS. The cells were spun down again at 600rcf for 5 minutes at 4°C. Now, the cells were transferred to the IgG-coated flask and incubated for 45 to 50 minutes to eliminate immune cell types which expressed the FcγR, which left behind an enriched population of T-cells suspended in media. This step was repeated once again to enrich the T-cell population further. The T-cells were pelleted down at 600rcf for 5 minutes and seeded in a 6-well plate with the appropriate cell number per well. They were then given the requisite activation and were maintained in IL2 (10 units/ml) to aid survival and proliferation.

PBMC Isolation from human blood

20 ml of blood was collected in sodium heparin tubes and diluted with PBS in a 1:1 ratio. It was layered with density gradient medium in a 2:3 ratio and centrifuged at 500rcf with an acceleration of 4 and deceleration of 0 at room temperature (RT) for 30 minutes. The buffy coat was isolated and washed with 10ml plain Rosewell Park Memorial Institute (RPMI) and then spun down at 500rcf for 10 minutes. This process was repeated once more to get rid of any leftover density gradient media. The isolated PBMCs were then counted and seeded in appropriate-sized plates/flasks. The cells were activated with either 25ng/ml Phorbol Myristate Acetate (PMA) and 0.5µM Ionomycin or 5µg/ml each of coated anti-CD3 and soluble anti-CD28. The cells were maintained in IL2 (10 units/ml) supplemented media and cultured at 37°C and 5% CO_2 for further experiments.

Biotinylation of Antibody

This process was done individually for every antibody. We took 1mg/ml of each antibody and then added 50µl of $NaHCO_3$ for every 0.5ml of Antibody solution. We added Ez-link sulfo-NHS biotin such that the ratio of moles of antibody to the moles of biotin is 1:20. These mixtures were incubated on the shaker for 2 hours, shielded from light at RT. The reaction was quenched using 1M Tris-base such that 2.5 µl of it was added for every 100 µl of biotin-antibody mixture. The separation columns were equilibrated with PBS once. Then, the biotinylated-antibody solution was washed 5 times with PBS through this separation column, and each time after washing, the separation column was spun down at 2000rcf at 4°C. To make the antibody cocktail, we mixed the biotinylated goat anti-mouse B220, CD4, IgG and CD16/CD32 in the ratio of 3:2:2:3. This was done to match the ratio of the corresponding cell populations, which bind to these specific antibodies and are found in splenic and lymph node isolates from mice (Veldkamp et al., 1974). For the positive human CD8+ T-cell isolation, we only used biotinylated mouse anti-human CD8 antibody.

Murine CD8+ T-cell isolation (Negative Selection)

We spun down 50 million cells and resuspended them in a falcon with 500µl of Magnetic Activated Cell Sorting (MACS) separation buffer. After adding 100µl of Fetal Bovine Serum (FBS) to this mixture, we added the biotinylated antibody cocktail such that its final concentration in the cell solution was 5 µg/ml. The FBS was added to prevent any non-specific binding of the antibody cocktail in the cell mixture. After this, we incubated the mixture for 15 mins on ice. At the end of this incubation, the volume of the cells-antibody mixture was made up with ice-cold PBS and the cells were spun down at 350rcf for 8 mins at 4°C. This wash was given to get rid of any unbound antibody that might be present in the solution. Subsequently, streptavidin-coated magnetic beads (stock concentration = 1.5×10^8 beads/ml) were mixed in with the biotinylated antibodies and cells such that the ratio of beads to cells was 4:1. Then the beads plus cells mixture was incubated for 15 mins at RT and was repeatedly mixed gently by swirling to allow biotin-streptavidin crosslinking. This suspension was transferred into a FACS tube, and the volume was made up to 3.5 ml with MACS buffer. After placing the FACS tube in the magnet, it was rotated gently a few times and then left undisturbed for 3 minutes. The solution was decanted into a falcon without removing the magnet. This helped separate out the CD8+ enriched fraction. After this, the FACS tube was removed from the magnet, and the bead-cell dimers were washed and

resuspended with MACS buffer. This fraction was the CD8+ depleted population of cells. Both these cell populations were spun down at 600rcf for 5 mins and cultured in IL-2 containing RPMI medium. The isolation efficiency was checked through flow cytometry by measuring the fraction of CD8+ cells in both these fractions as well as the pre-sorted fraction of cells. In the subsequent times that murine CD8+ isolation was done, the CD8+ depleted population was discarded, and the enriched population was activated and cultured for further experiments.

Human CD8+ T-cell isolation (Positive Selection)

We started with 10 million PBMCs and resuspended them in 200 µl of MACS buffer in a falcon. To this, we added biotinylated mouse anti-human CD8+ antibody such that the final concentration of it in the cell solution was 5 µg/ml. This mixture was incubated at RT for 10 mins. Streptavidin-coated magnetic beads (stock concentration = 1.5 x 10^8 beads/ml) were added to the cell antibody mixture such that the ratio of beads to cells was 1:1. Now, this bead antibody cell mixture was incubated at RT for 5 mins. Once the incubation was over, the entire contents were transferred into a FACS tube where the volume was made up to 3.5 ml with MACS buffer. The FACS tube was placed in the magnet, rotated gently a few times and then left undisturbed for 5 minutes. Subsequently, the solution was decanted into a falcon without removing the magnet. This flowthrough was the CD8+ depleted fraction. Now, the FACS tube was taken out of the magnet, and the bead-cell dimers were washed and resuspended with MACS buffer. This solution contained the CD8+ enriched fraction. Both these cell populations were spun down at 600rcf for 5 mins and cultured in IL2 containing RPMI. The isolation efficiency was checked through flow cytometry by measuring the fraction of CD8+ cells in both these fractions as well as the pre-sorted fraction of cells. In the subsequent times that human CD8+ isolation was done, the CD8+ depleted population was discarded, and the enriched population was activated and cultured for further experiments.

Flow cytometry to check CD8+ isolation/antibody biotinylation efficiency

We checked the CD8+ isolation efficiency by staining with Fluorescein isothiocyanate (FITC) labelled anti-mouse CD8 antibody and Pacific Blue anti-human CD8 antibody. We used 50µl of staining solution for 0.1 million cells. To check the biotinylation efficiency of the antibody, we stained with fluorescently labelled streptavidin beads. Post-staining, the protocol for both these experiments was the same. We washed the cells twice with flow

buffer and then spun them down at 520rcf for 6 mins. After discarding the supernatant, we fixed the cells in 3.7% Paraformaldehyde (PFA) for 20 mins at RT. These cells were then stored at 4°C until they were taken for flow cytometry.

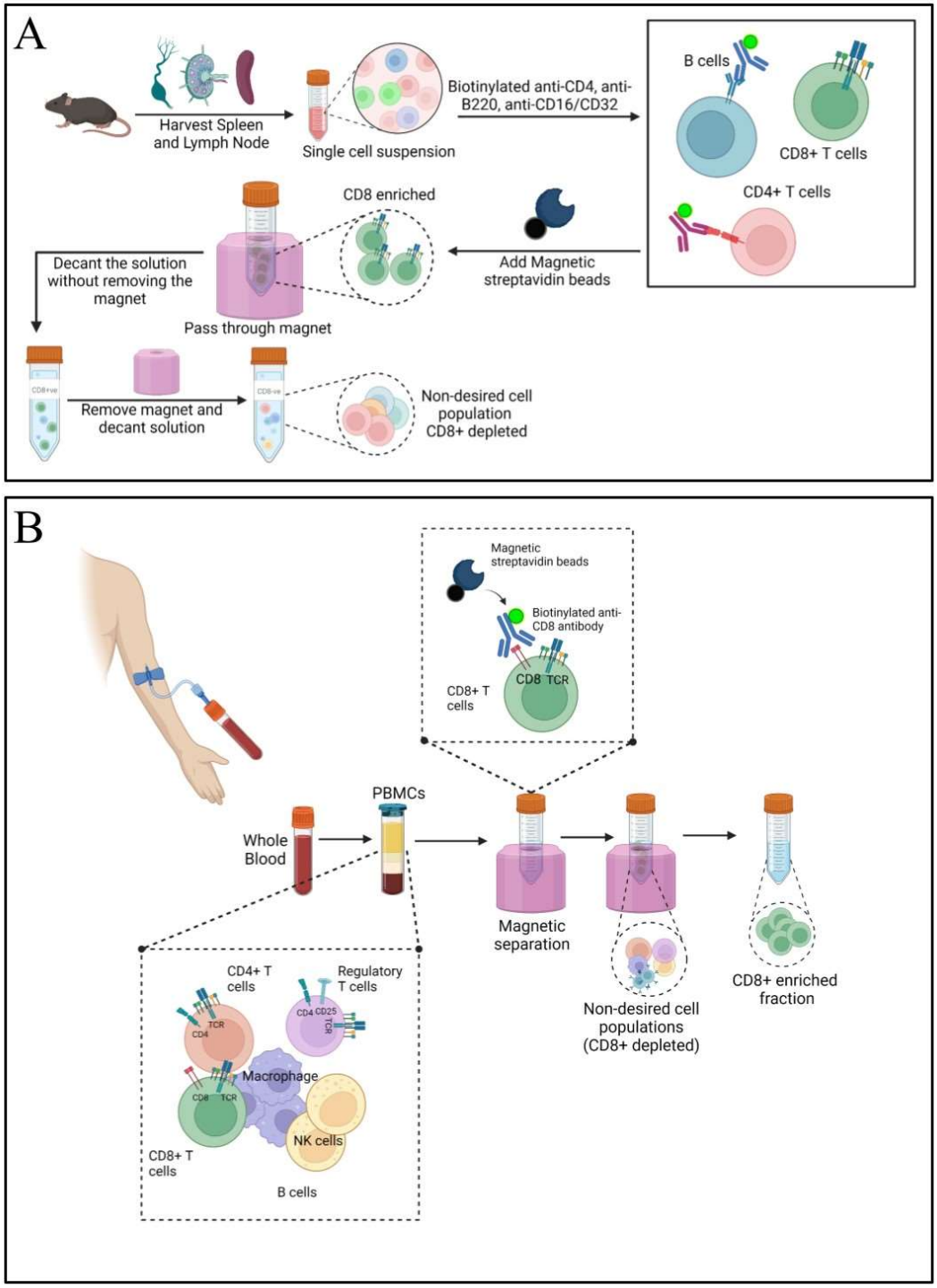

Figure 10 - CD8+ T-cell isolation outline for (A) Mice and (B) Humans (Biorender.com)

Drug treatment (*)

CK666 – No pretreatment, 100 µM for the duration of the experiment across all experiments.

U-Drug – Pretreatment of 1µM for 30 minutes across all experiments.

MβCD – Pretreatment of 5µM for 5 mins during filipin staining. No pretreatment, 0.9 µM for the entire duration of the CTL degranulation assay and the cytotoxicity assay.

Cell Activation conditions

In Degranulation and Cytotoxicity assay experiments, the isolated CD8+ T-cells were primed/activated using one of two methods. In the first method, CD3-CD28 based activation was carried out where the cells were incubated in wells coated with 5 µg/ml anti-CD3 along with 5 µg/ml soluble anti-CD28 in the media overnight. Then, these cells were rested for 48 hours in IL-2 containing RPMI and used for further experiments. In the second method, the cells were stimulated with 25ng/ml of PMA and 0.5µM of ionomycin both dissolved in RPMI media. After overnight stimulation, they were rested for 48 hours, and then the cells were used for further experiments.

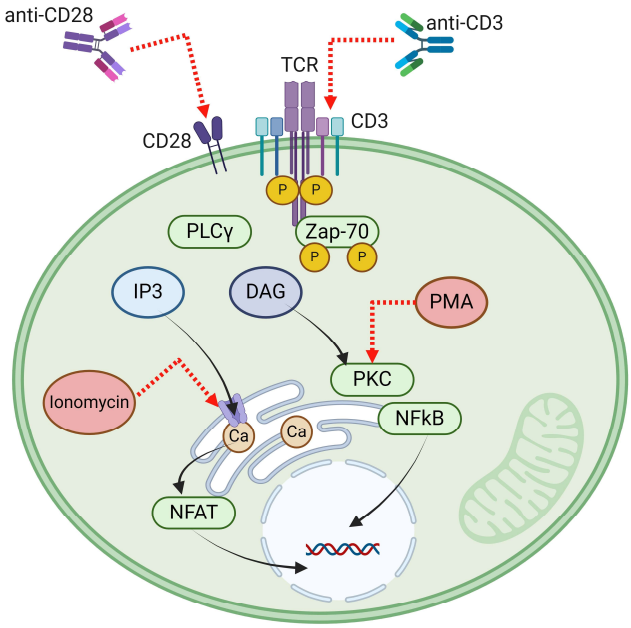

Figure 11- Schematic representing the activation of CTLs in 2 ways. One with anti-CD3 and anti-CD28, the other with PMA and Ionomycin (Biorender.com)

Filipin Staining

Cells were fixed with 3.7% PFA for 20 mins at room temperature (RT). After rinsing them with phosphate buffer saline (PBS) thrice, they were stained with 0.05mg/ml filipin for 1 hour at RT. Once again, the cells were washed thrice with PBS, resuspended in flow buffer, and viewed by epifluorescence microscopy using a UV filter set (340-380 nm excitation, 40 nm dichroic, 430 nm long pass filter). The same protocol is used for staining in microscopy chambers as well.

Note:

1. Protect Filipin solutions from light. Filipin is very light-sensitive and undergoes rapid photobleaching.
2. This protocol has been adapted from the Tabas Laboratory ("Ira Tabas, MD, PhD, Columbia University," n.d.)

CTL Degranulation Assay

We took the CD8+ activated cells and kept them in IL-2-free media overnight. 2 hours before the experiment, we put them for serum starvation to prevent any non-specific premature degranulation due to proteins that are already present in the media. Then, we treated the cells with CK666, U-Drug and MβCD. The specific conditions of drug treatment that were used have been mentioned previously (*). These pretreated cells were then further stimulated to degranulate in two separate ways. In the first condition, a well coated with 5 µg/ml of anti-CD3 was used along with 5 µg/ml of soluble anti-CD28 in the media. In the second condition, 25 ng/ml of PMA was used along with 0.5 µM/ml of ionomycin. After this, we added 2µg/ml of Phycoerythrin (PE) labelled LAMP-1 antibody in case of human CTLs and Alex Fluor 647 in case of murine CTLs and incubated at 37°C for 1 hour. Then, we added 100ng/ml Brefeldin (golgi stop) to freeze Golgi movement and transport and prevent internalisation of any LAMP-1 that has been tagged on the cell's surface. We incubated at 37°C for another hour. Finally, we fixed the cells with 3.7% PFA for 20 mins at RT. The cells were stored at 4°C until they were taken for flow cytometry. The percentage of the parent population was measured for LAMP-1 (660nm) and compared across the various drug conditions. The plate set up for the experiment is given in Figure 11.

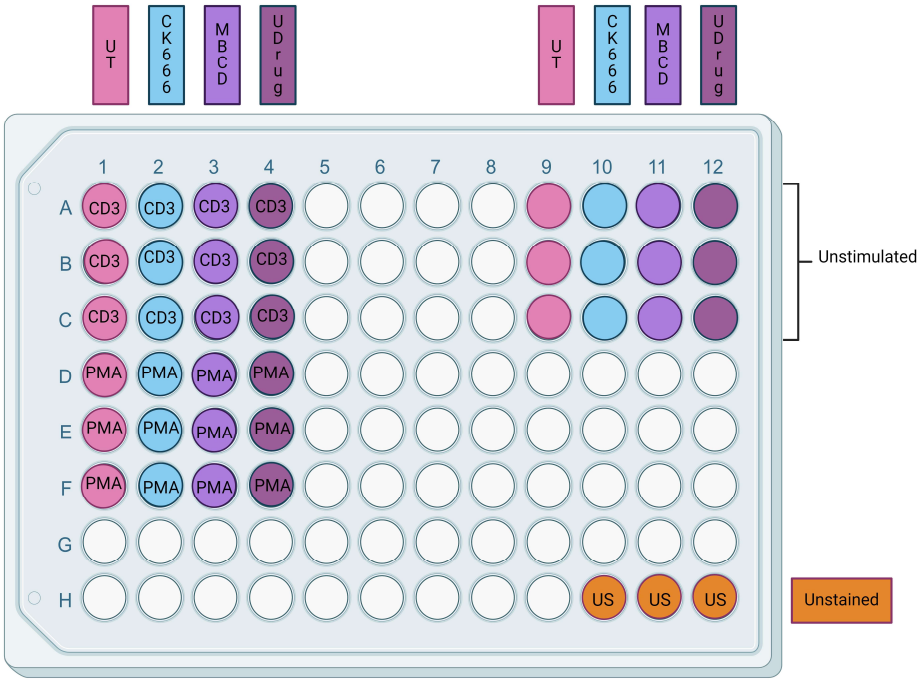

Figure 12 - Plate Layout for Degranulation Assay. UT = Untreated, US = Unstained, CD3 = Stimulated with anti-CD3 and anti-CD28, PMA = Stimulated with PMA and ionomycin (Biorender.com)

Granzyme B staining synapse experiment

We carried out a synapse imaging experiment where we took primary mouse primed CD8+ T-cells and looked at their actin intensity and features along with granzyme content under 2 synapse timepoints - 2 mins and 10 mins. We coated pre treated 8 well imaging chambers with 5µg/ml of mouse anti-CD3 antibody and 2 µg/ml of ICAM-1 overnight. Subsequently we treated the cells with CK666, U-Drug and MβCD. The specific conditions of drug treatment that were used have been mentioned previously (*). 0.1 million cells were added per well for the 10 min synapse and 0.5 million cells were added for the 2 min synapse. This proportion was used in order to get uniform distribution of cells in each well. All the cells were immediately fixed with 3.7% PFA for 20 mins at RT to arrest the synapse dynamics at 2 and 10 mins. They were then permeabilized using 0.2% Tween 20 for 20 mins at RT. The reason for using Tween 20 and not Triton X 100 was that Tween is a milder detergent and it doesn't disrupt cholesterol content of the cell. Since, we also wanted to do Filipin staining to mark the cholesterol, we chose to use Tween. After permeabilization, the cells were incubated overnight at 4°C with Alexa Fluor 488 Phalloidin and Alexa Fluor 647 anti-human/mouse Granzyme B antibody. Phalloidin binds to F-actin polymers and thus its stains

the actin architecture of the cell. The granzyme B antibody stains granzyme B molecules present in cytotoxic granules that are present within the cells and haven't degranulated. The next day the cells were washed twice with PBS and then filipin staining was done as mentioned before. 100X epifluorescence imaging was carried out where actin was visualised with the help of phalloidin under the FITC channel, Granzyme B was seen with the help of Cyanine 5 (Cy5) channel and the Filipin staining was visualised with the help of the DAPI channel.

Figure 13 – 8 well chamber layout for the Granzyme B synapse timepoint experiment. (Biorender.com)

Image Analysis

All the image analysis was done using ImageJ for quantifying cholesterol in different treatment conditions. ROI drawing was done for every field by virtue of thresholding. The mean fluorescence intensity was measured for all the cells in each condition and was then plotted to compare the differences between the various treatment conditions.

Flow cytometry Analysis

All the flow cytometry analysis was done using FlowJo version 10.8.1 for analysing degranulation assay. It was also used to look at the CD8+ T-cell isolation purity and the biotinylation of the antibody.

Statistics

All the statistical tests were done using GraphPad Prism 8.0. Parametric unpaired students' T-tests were done to look at the significance of the epifluorescence data from the filipin staining as well as the synapse plate experiment. All the flow cytometry data was analysed by non-parametric unpaired T-tests.

Results

Verifying the effect of MβCD and U-Drug on cell membrane cholesterol levels.

We saw a clear difference in the cholesterol levels present on the cell membrane of T-cells, which were treated with MβCD and U-Drug. Epifluorescence images were captured at 30X using Olympus IX83 for quantification. Representative images have been shown at 100X in Figure 13. The whole cell mean fluorescence intensity (MFI) was analysed for over 500 cells in each condition. As expected, MβCD depleted the cholesterol levels in the cell membrane as shown in previous studies (Mahammad and Parmryd, 2015; Zidovetzki and Levitan, 2007). U-Drug on the other hand saturated the cholesterol levels as expected (Cenedella, 2009; Lu et al., 2015; Salata et al., 2017). Analysis was done by parametric unpaired students' T-test.

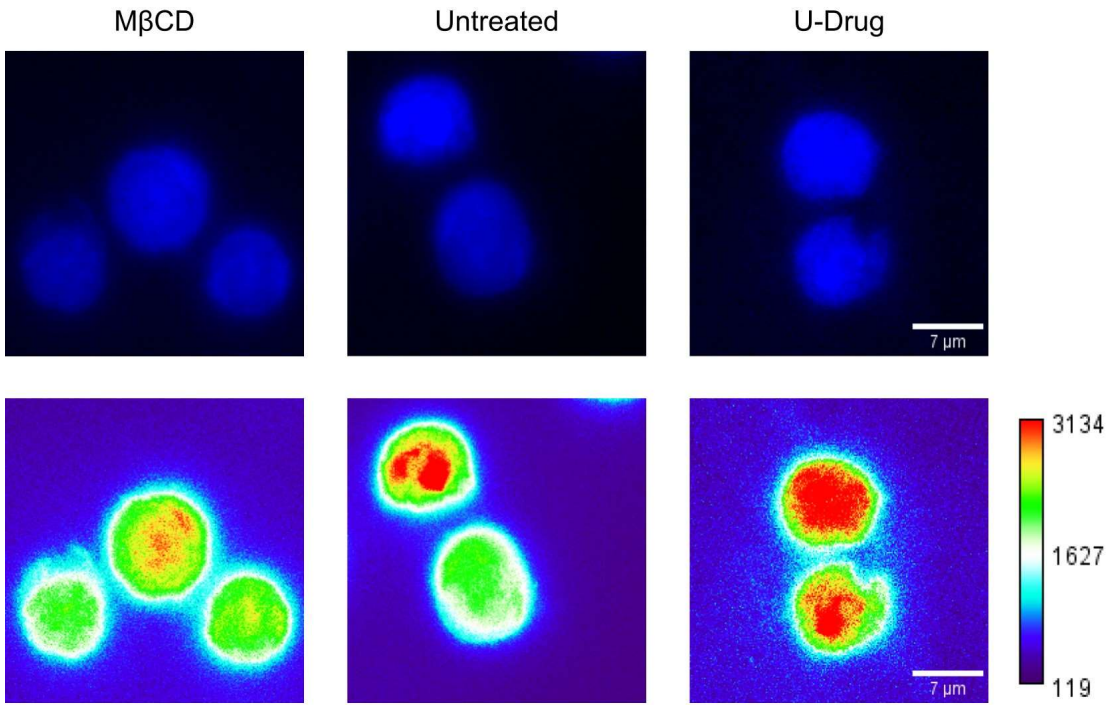

Figure 14 - 100X epifluorescence microscopy images of cells treated with MβCD & U-Drug. Upper panel = Representative images of the three conditions. Lower Panel = Images converted into thermal scale in order to highlight the contrast.

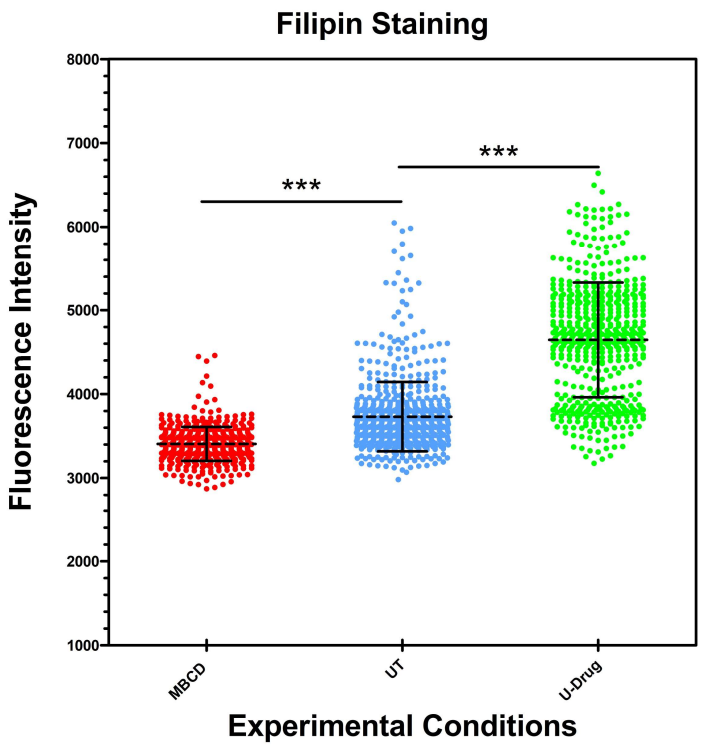

Figure 15 - Comparison of MFI of cells across the three conditions. Significance analysis done by parametric unpaired students' T-test (n ≥ 500).

Checking biotinylation of antibodies used for murine CD8+ T-cell isolation

We carried out flow cytometry to check if the biotinylation of the antibody had worked before proceeding with the murine CD8+ T cell isolation. We checked for individual antibody-labelled populations of immune cells from single cell suspension of lymph nodes and splenic isolates of mice. We did this by incubating separate tubes of cells with biotinylated antibodies and then checked for the number of cells that were labelled with the antibody using fluorescently labelled streptavidin.

Biotinylation of the anti-CD4 antibody had worked since the number of cells it was binding to was comparable to the physiological number of CD4+ T-cells found in the spleen and lymph nodes. This was also observed for IgG which marks B-cells. Thus, we saw that the percentage of labelled cell populations were comparable to numbers reported in studies done previously (Nolte et al., 2000) and concluded that the biotinylation of the antibodies was successful. The percentage of parent plots for each antibody are shown in figure 14 along with a plot depicting the physiological numbers of the different immune cells found in the mouse spleen and lymph nodes (Nolte et al., 2000).

Checking the biotinylation of the anti-human CD8 antibody couldn't be carried out since the physiological numbers for CD8+ T-cells vary drastically for each individual (Sender et al., 2023).

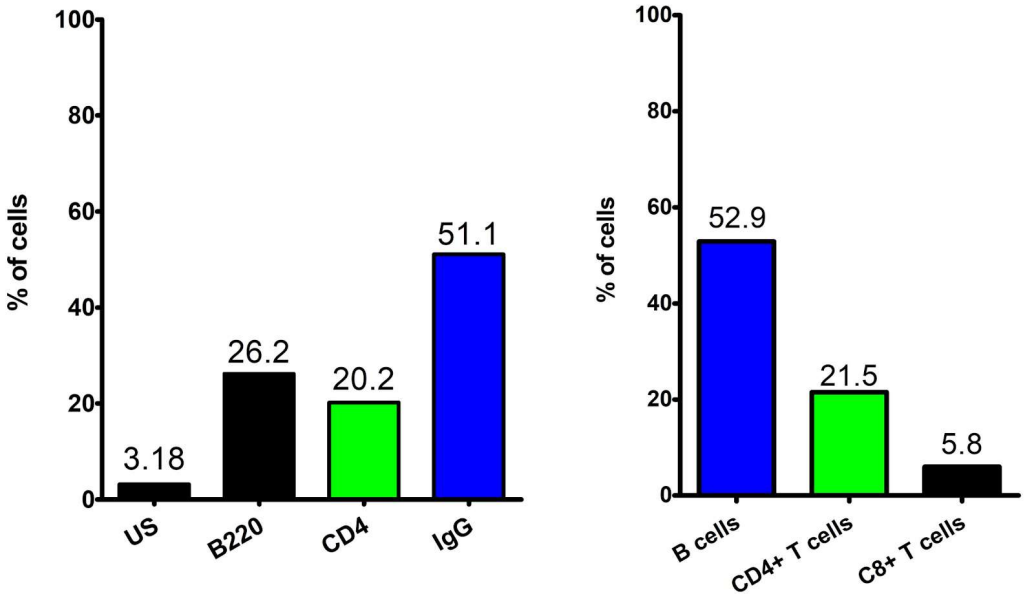

Figure 16 - Left Graph = Biotinylated antibody labelled cells checked with fluorescent streptavidin beads. Right Graph = Representative data from a study that estimates the amount and distribution of the various immune cell types in the spleen and lymph nodes (Nolte et al., 2000). The bars indicated in blue and green are the ones that should be compared.

Checking the efficiency of CD8+ T-cell isolation

Human

We checked the efficiency of human CD8+ T-cell isolation through flow cytometry. We did this by staining for CD8+ T-cells in the enriched and depleted fractions as well as the pre-sorted fraction. The samples were stained using a Pacific Blue (PB) anti-human CD8 antibody as well as Brilliant Ultra Violet (BUV) 661 anti-human CD3 antibody. The cells that were double positive (CD3+ and CD8+) were considered, as CTLs express both the ligands on their cell surface (Charles A Janeway et al., 2001e). There was a significant increase in CD8+ T-cell proportion within the CD8 enriched fraction when compared with the whole PBMC fraction. Analysis was carried out using non-parametric unpaired T-test. Our homemade kit gave an efficiency of around 75 - 80%. The commercial kit on the other hand claimed an efficiency of around 90 - 95% ("Human CD8+ T Cell Isolation - IN," n.d.)

and was significantly more expensive. As there wasn't a drastic difference between the isolation efficiencies of the homemade V/s the commercially available kit, we continued to use the inhouse method for future experiments. Standardization of this protocol was carried out in the lab. The experiment was repeated 3 times to test validity.

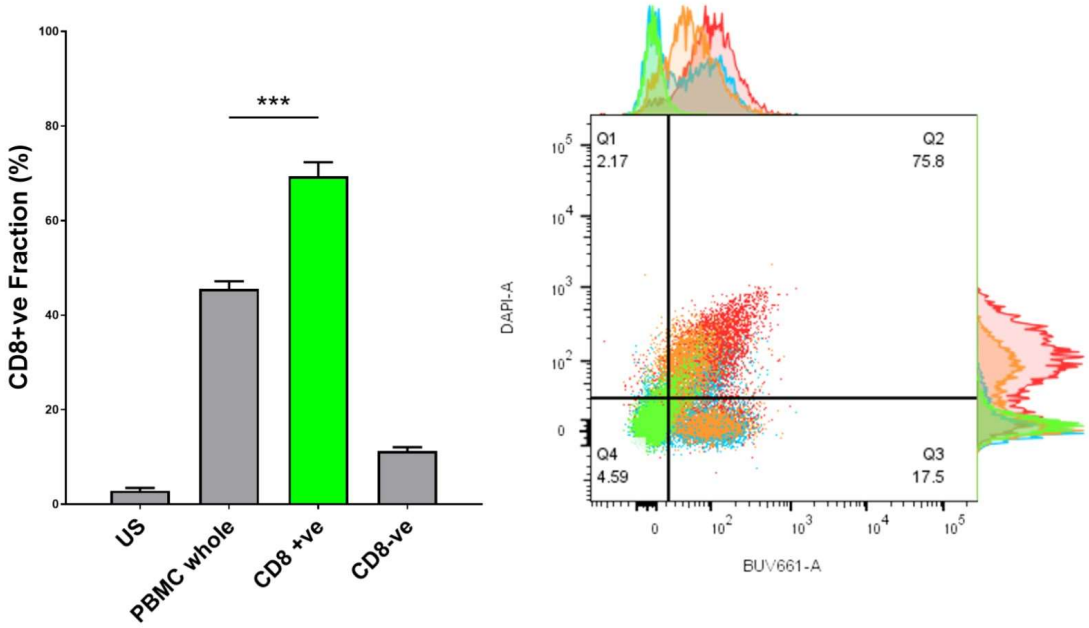

Figure 17 - Flow cytometry data for checking human CD8+ T-cell enrichment after isolation with the homemade kit. Left Graph = Percentage CD8 T-cell fraction seen in Unstained (US), whole PBMCs, CD8+ves and CD8-ves. Significance was checked by paired students' T-test. Right Graph = Dot plot showing single replicates of all the fractions from the left graph and their spread across a 2D space formed by the 2 antibody stains (n = 3).

Mouse

After checking for the biotinylation of the antibodies and making the antibody cocktail, we carried out the CD8+ T-cell isolation and checked for its efficiency. Through flow cytometry we checked for the fraction of CD8 T-cells in the CD8 enriched and depleted fractions as well as the pre-sorted fractions as done previously in the case of human isolation. Flow cytometry data of the different fractions was obtained using FITC anti-mouse CD8 antibody. We compared the isolation efficiency from the homemade kit with the efficiency of isolation of a commercially available kit that we had ("Dynabeads™ Untouched™ Mouse CD8 Cells Kit," n.d.). The plots for both of these experiments are shown in Figure 18 and 19. Both the kits showed a significant increase in CD8+ve fraction in the CD8 enriched V/s the presorted populations. Analysis was carried out using non-parametric unpaired T-test.

The commercial kit gave us an efficiency of around 80 - 85% whereas the homemade kit gave us an efficiency of around 70 - 75%. Since the difference between the two wasn't too large and the homemade kit was significantly more cost effective, we continued to use it for further experiments. Similar to the Human isolation kit, standardization of this protocol was also carried out in the lab. These experiments were replicated twice to check validity.

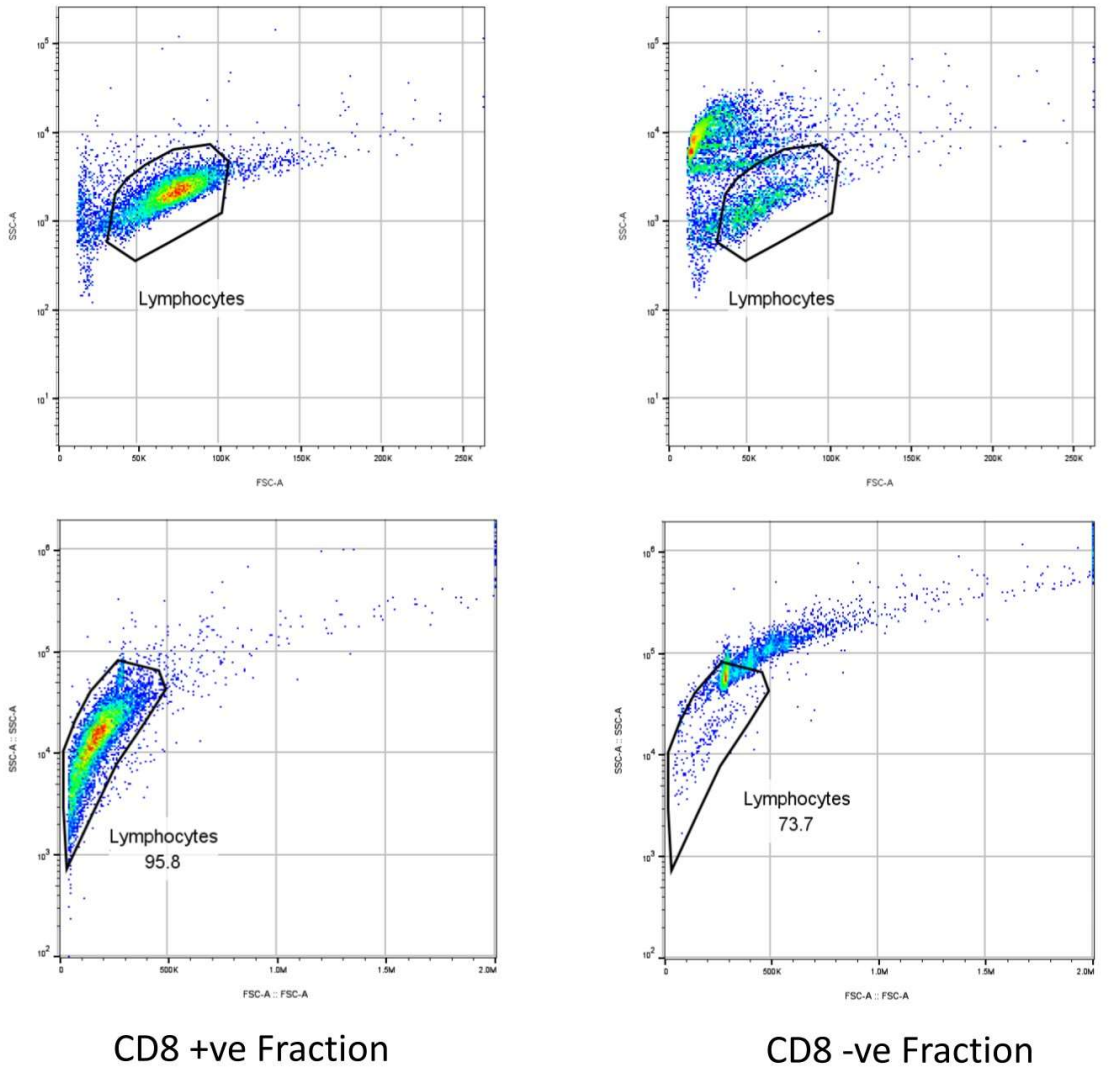

Figure 18 - Representative SSC V/s FSC plots for the CD8 enriched (CD8+ve) and the CD8 depleted (CD8-ve) fractions showing the distribution of cells. The top panel is for the commercial kit isolation and the bottom panel is for the homemade kit isolation. You can clearly see the enriched lymphocyte population in the positive fraction which is absent in the negative fraction.

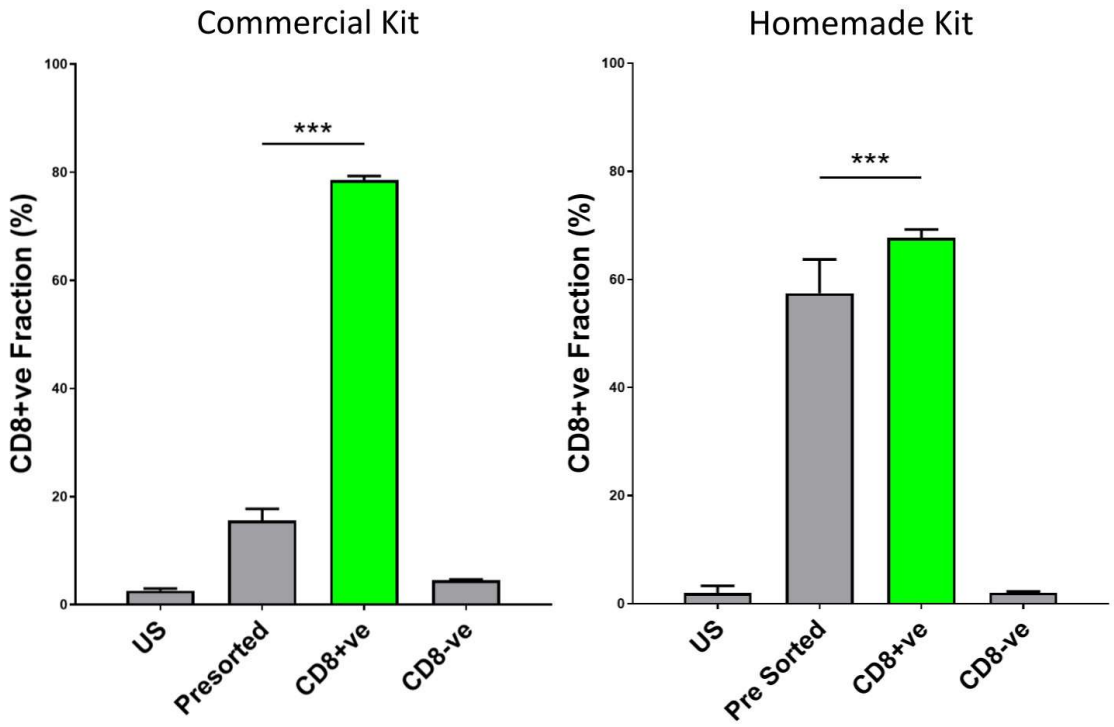

Figure 19 - Data for checking efficiency of mouse CD8+ T-cell isolation using the commercial kit and the homemade kit. In both the graphs, there are the Unstained (US), Pre-sorted, CD8+ve and CD8-ve fractions. Significance analysis carried out by non-parametric unpaired T-test (n = 2).

Effect of cholesterol perturbation on degranulation in CTLs

Human and murine CD8+ T-cells after isolation using homemade kits were primed with PMA and Ionomycin and used for the degranulation assay. The extent of degranulation was detected with the help of the proportion of cells that were LAMP-1 positive. Changes in the frequency of the parent population were measured across various activation and treatment conditions to see if the small molecule inhibitors did in fact have an effect on the extent of degranulation. Figures 20 and 21 contain the data for the extent of degranulation in human CTLs. There was no significant change observed in the extent of degranulation after treatment with the inhibitors. The same was observed for murine CTLs as shown in the figures 22 and 23. The experiment was repeated once both in case of murine as well as human CTLs to test validity. The protocol for degranulation assay was standardized for the lab.

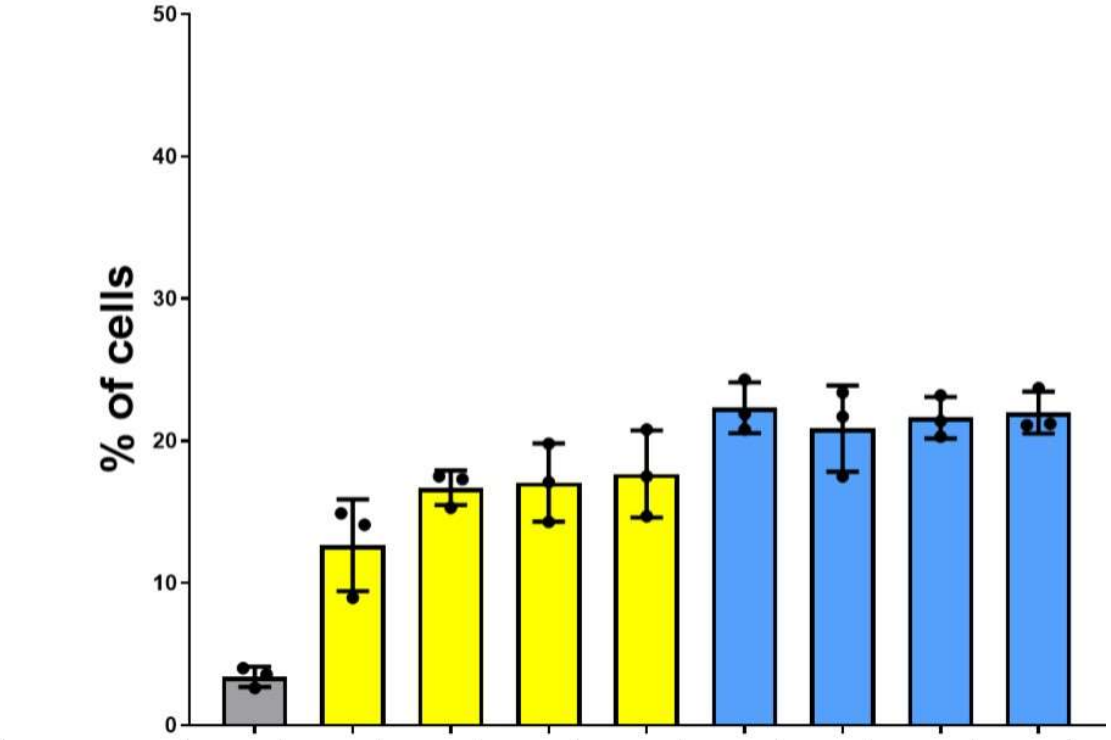

CD3 + CD28	-	-	-	-	-	+	+	+	+
PMA + Iono	-	-	-	-	-	-	-	-	-
CK666	-	-	+	-	-	-	+	-	-
MBCD	-	-	-	+	-	-	-	+	-
U-Drug	-	-	-	-	+	-	-	-	+

Figure 20 - Degranulation assay data for human CTLs activated with anti-CD3 and anti-CD28. The frequency of parent was plotted on the Y axis along with the various treatments and activation conditions on the X axis. The difference in degranulation between conditions were non-significant. Significance was checked using non-parametric unpaired T-test. (n = 2)

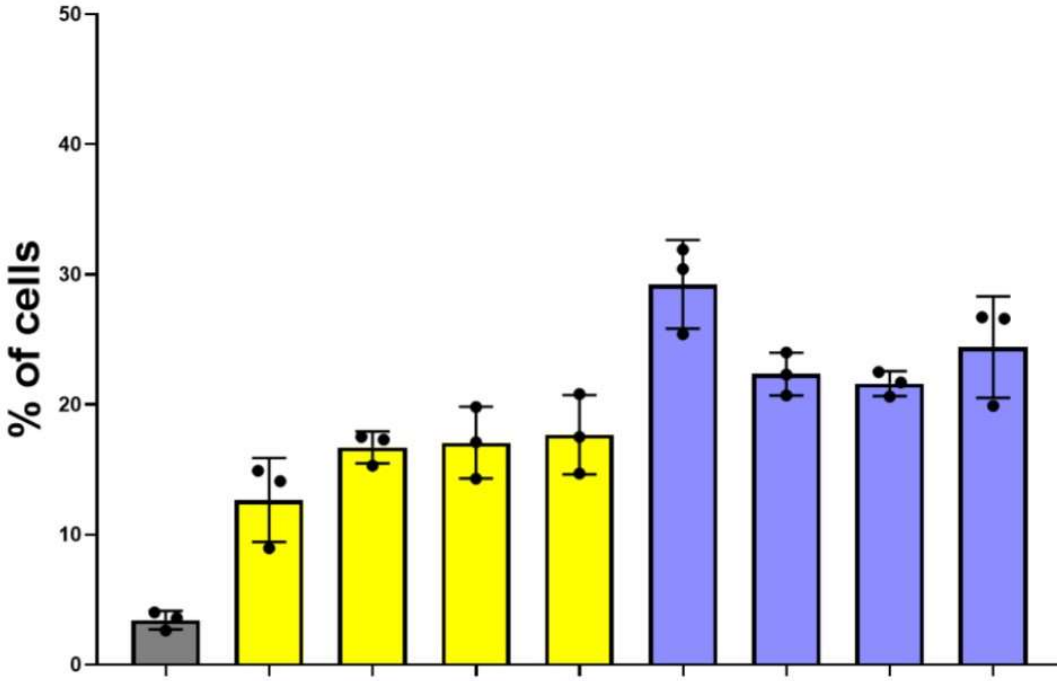

CD3 + CD28	-	-	-	-	-	-	-	-	-
PMA + Iono	-	-	-	-	-	+	+	+	+
CK666	-	-	+	-	-	-	+	-	-
MBCD	-	-	-	+	-	-	-	+	-
U-Drug	-	-	-	-	+	-	-	-	+

Figure 21 – Degranulation assay data for human CTLs activated with PMA and Ionomycin. The frequency of parent was plotted on the Y axis along with the various treatments and activation conditions on the X axis. The difference in degranulation between conditions were non-significant. Significance was checked using non-parametric unpaired T-test. (n = 2)

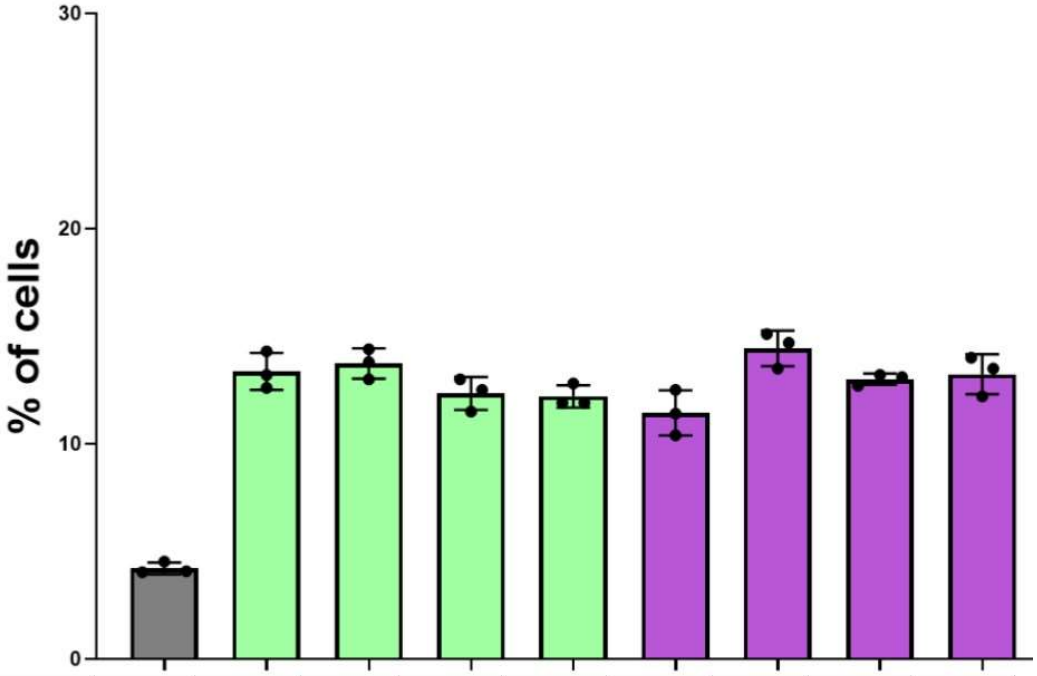

CD3 + CD28	-	-	-	-	-	-	-	-	-
PMA + Iono	-	-	-	-	-	+	+	+	+
CK666	-	-	+	-	-	-	+	-	-
MBCD	-	-	-	+	-	-	-	+	-
U-Drug	-	-	-	-	+	-	-	-	+

Figure 22 - Degranulation assay data for murine CTLs activated with PMA and Ionomycin. The frequency of parent was plotted on the Y axis along with the various treatments and activation conditions on the X axis. The difference in degranulation between conditions were non-significant. Significance was checked using non-parametric unpaired T-test. (n = 2)

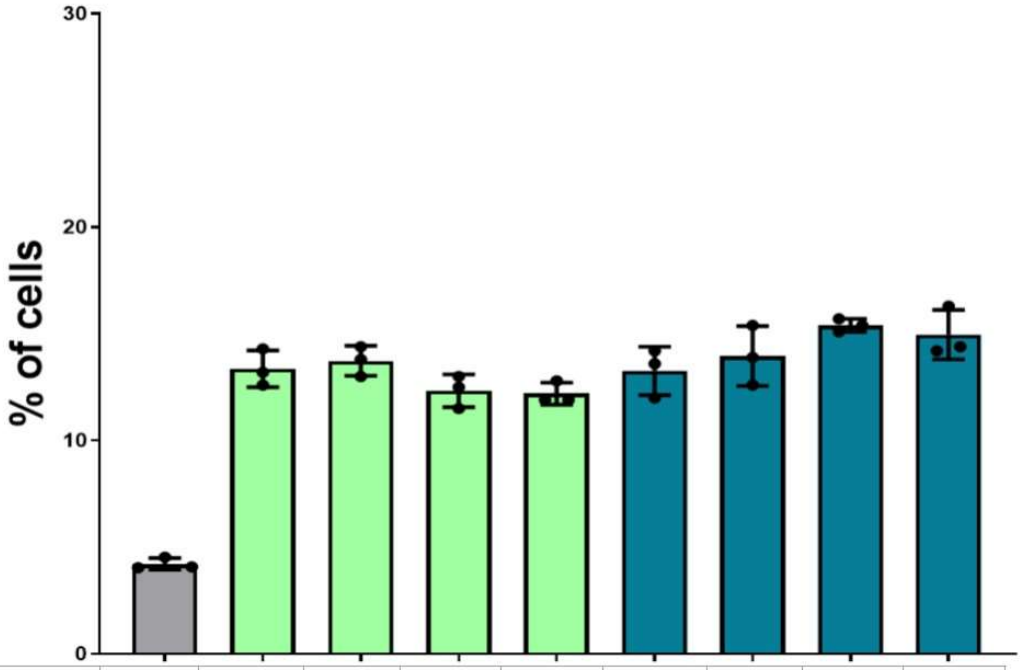

CD3 + CD28	-	-	-	-	-	+	+	+	+
PMA + Iono	-	-	-	-	-	-	-	-	-
CK666	-	-	+	-	-	-	+	-	-
MBCD	-	-	-	+	-	-	-	+	-
U-Drug	-	-	-	-	+	-	-	-	+

Figure 23 - Degranulation assay data for murine CTLs activated with anti-CD3 and anti-CD28. The frequency of parent was plotted on the Y axis along with the various treatments and activation conditions on the X axis. The difference in degranulation between conditions were non-significant. Significance was checked using non-parametric unpaired T-test. (n = 2)

Multiple studies have reported multi-fold increases in the percentage of the parent population as well as the median fluorescence intensity during their degranulation assays when they quantified LAMP-1 expression on the cell surface (Lorenzo-Herrero et al., 2019; Terrén et al., 2023; Weigelin et al., 2021). As we don't see such a stark difference, we conclude that cholesterol might not play as large a role in controlling the release of cytotoxic granules as it might play modulating CTL activity through various other pathways.

Effect of CK666, MβCD and U-Drug on cytotoxic granules and actin

Since we couldn't see any changes in the degranulation extent of CTLs after treating with these pharmacological inhibitors. We thought it would be worthwhile to see if there was granular accumulation in the T-cells that these drugs were causing. We looked at the actin architecture during synapse formation as a control since others in the lab had already looked at the effect of some of these drugs on the actin framework during synapse formation. The cells were allowed to synapse for a short duration and a longer duration. 2 minutes was chosen to observe the early synapse properties of the cells. 10 minutes on the other hand is a long time in terms of synapse progression and was chosen to visualise the properties of the cells stabilizing the synapse. The mean fluorescence intensity was measured for cells across various conditions and plotted. Significance analysis was carried out by students' T-test.

There was no significant change observed in the amount of granzyme B staining across all the conditions in both the 2minute and 10minute synapsing cells. This implied that none of these drugs caused the stagnation of cytotoxic granule transport or granule accumulation in primed CTLs. The presence of granules was confirmed visually as punctate structures within the cells as have also been shown in the representative images in figure 25. Although the proportion of cells that were positive for granzyme staining were relatively less. This could be due to the fact that the primed CTLs might be degranulating due to external stimulation from certain media components. Thus, although previously in the lab it had been shown that MβCD and CK666 slow down granular movement within the cell. They don't seem to stagnate it and they certainly are not causing accumulation of granules.

Analyzing the phalloidin staining data, CK666 caused a reduction in the mean phalloidin intensity as compared to the Untreated (UT) cells both in the 2minute and 10minute case. Phalloidin binds to F-actin polymers and thus reduction in its intensity implies that the amount of F-actin is going down in the cell. This is a widely observed phenotype and the

molecular mechanism behind this has also been studied (Henson et al., 2015; Hetrick et al., 2013).

An interesting point to note is that in the 2minute synapse, U-Drug was also causing a reduction in the mean fluorescence intensity but that difference disappeared at the 10minute timepoint. This however was not observed when the experiment was repeated and thus could be due to a handling error.

The trends seen in filipin fluorescence intensity were conserved and were identical to the variation seen in the first result described. CK666 did not change the cellular cholesterol content and thus showed a non-significant change when compared to the untreated cells.

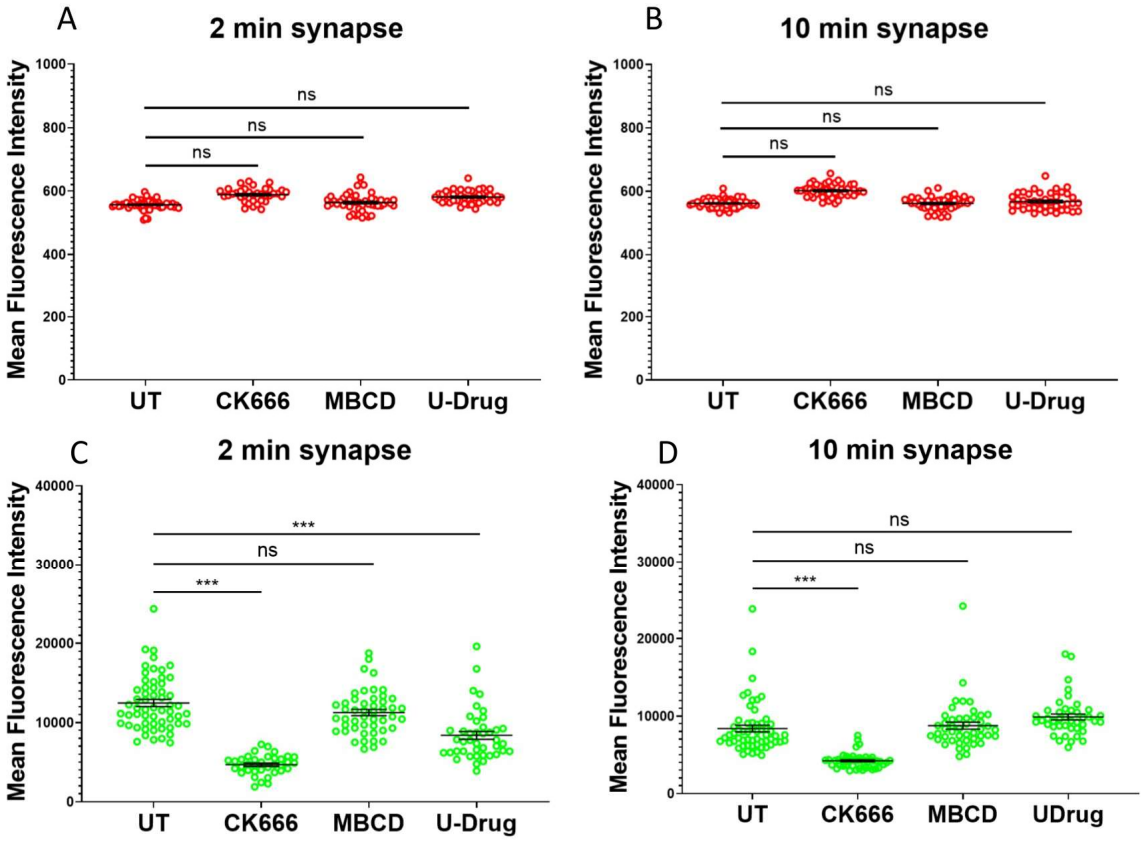

Figure 24 - Scatter Plots depicting the variation in mean fluorescence intensity for granzyme B (A & B) as well as Phalloidin (C & D). Graphs A & B show the variation in Granzyme B levels across different treatment conditions after 2minute and 10minute synapses respectively. Graphs C & D show the variation in Phalloidin stained actin levels across different treatment conditions after 2minute and 10minute synapses respectively. Significance analysis was carried out using students' T-test. (n = 2)

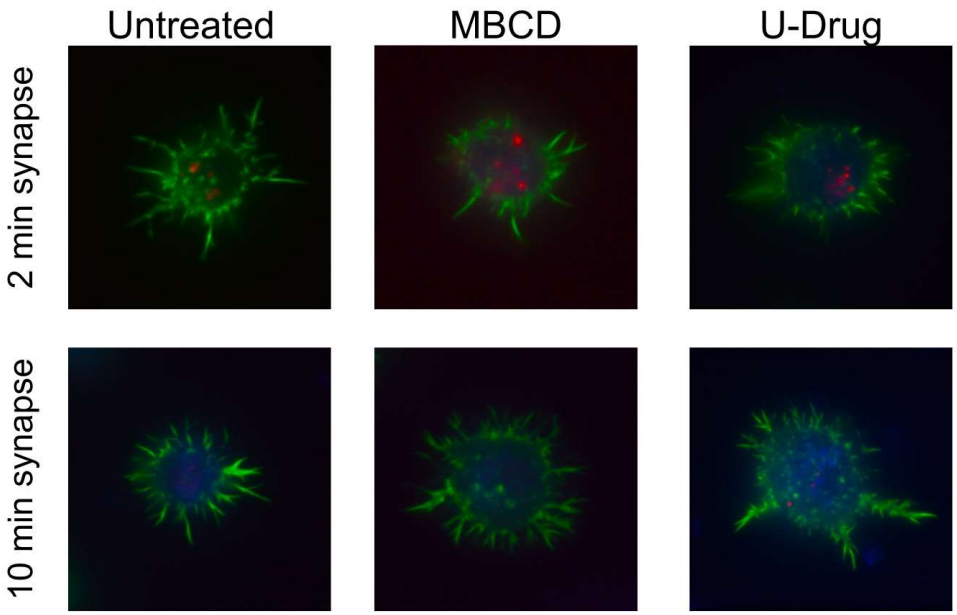

Figure 25 – A panel of representative images of cells from each treatment condition for both the 2minute synapse and the 10minute synapse. The green channel is for Phalloidin 488 which stains F-actin. The red channel is for Granzyme B and the blue channel is for Filipin III which stains membranous cholesterol in the cell.

Discussion

The work focussed on studying the effect of cell membrane cholesterol on degranulation in cytotoxic T-cells. The data gathered confirmed that MβCD and U-Drug both do in fact work antagonistically to modulate the cholesterol concentrations of the membrane of the cell. Their mechanisms of action and effects have been shown in multiple scenarios and they do behave in a similar manner when it comes to T-cells as well (van Gestel et al., 2005) (Mahammad and Parmryd, 2008). Although both these drugs have other effects on the cells as well, by optimizing their concentrations and the time of treatment, we have been able to minimize undesired effects in order to mimic conditions that we require to study the effect of cholesterol in the cell membrane and how it can affect degranulation.

We standardized the CD8+ isolation protocols for both murine and human models. Our primary motive to do this was to make the process of CD8+ T-cell isolation cost effective and efficient.

As it was seen previously, MβCD and U-Drug both affected endosomal movement within the cell prior to degranulation. However, MβCD and U-Drug did not have an effect on the extent of degranulation in both human and murine CTLs. Even across different activation and priming conditions for the CTLs, we didn't see any significant change. This hints to the fact that maybe the processes of granule movement and degranulation might be decoupled and aren't completely dependent on each other. This implies that the movement of the granules towards the synapse is not necessarily a rate limiting step for degranulation and there might be prior accumulation of granules over a period of time before the cell decides its ready to degranulate (Anikeeva and Sykulev, 2011). Granules accumulation and degranulation might be governed by separate mechanisms. This is in keeping with the multiple hit theory of T-cell degranulation. This theory assumes that you require more than a certain threshold of granules to cause target cell killing and hence it benefits to have granule accumulation in the T-cell in order to ensure effective target cell killing.

We also observed that these drugs didn't lead to stagnation of granule transport nor did they cause abnormal granule accumulation in CTLs which was checked by virtue of Granzyme B staining.

Thus these studies provided major insights into into the effect of degranulation and the role that the cholesterol present in the cell membrane plays in the process.

References

Immunity - Quick search results | Oxford English Dictionary. https://www.oed.com/search/dictionary/?scope=Entries&q=immunity.

Immunization - Quick search results | Oxford English Dictionary. https://www.oed.com/search/dictionary/?scope=Entries&q=immunity.

Angus, K.L., Griffiths, G.M., 2013. Cell polarisation and the immunological synapse. Current Opinion in Cell Biology, Cell architecture 25, 85–91. https://doi.org/10.1016/j.ceb.2012.08.013

Anikeeva, N., Sykulev, Y., 2011. Mechanisms Controlling Granule-mediated Cytolytic Activity of Cytotoxic T Lymphocytes. Immunol Res 51, 183–194. https://doi.org/10.1007/s12026-011-8252-8

Broere, F., van Eden, W., 2019. T Cell Subsets and T Cell-Mediated Immunity, in: Parnham, M.J., Nijkamp, F.P., Rossi, A.G. (Eds.), Nijkamp and Parnham's Principles of Immunopharmacology. Springer International Publishing, Cham, pp. 23–35. https://doi.org/10.1007/978-3-030-10811-3_3

Cassioli, C., Baldari, C.T., 2022. The Expanding Arsenal of Cytotoxic T Cells. Front. Immunol. 13. https://doi.org/10.3389/fimmu.2022.883010

Cenedella, R.J., 2009. Cholesterol Synthesis Inhibitor U18666A and the Role of Sterol Metabolism and Trafficking in Numerous Pathophysiological Processes. Lipids 44, 477–487. https://doi.org/10.1007/s11745-009-3305-7

Charles A Janeway, J., Travers, P., Walport, M., Shlomchik, M.J., 2001a. The Humoral Immune Response, in: Immunobiology: The Immune System in Health and Disease. 5th Edition. Garland Science.

Charles A Janeway, J., Travers, P., Walport, M., Shlomchik, M.J., 2001b. Principles of innate and adaptive immunity, in: Immunobiology: The Immune System in Health and Disease. 5th Edition. Garland Science.

Charles A Janeway, J., Travers, P., Walport, M., Shlomchik, M.J., 2001c. Summary to Chapter 1, in: Immunobiology: The Immune System in Health and Disease. 5th Edition. Garland Science.

Charles A Janeway, J., Travers, P., Walport, M., Shlomchik, M.J., 2001d. T cell-mediated cytotoxicity, in: Immunobiology: The Immune System in Health and Disease. 5th Edition. Garland Science.

Charles A Janeway, J., Travers, P., Walport, M., Shlomchik, M.J., 2001e. Antigen recognition by T cells, in: Immunobiology: The Immune System in Health and Disease. 5th Edition. Garland Science.

Dustin, M.L., 2014. The immunological synapse. Cancer Immunol Res 2, 1023–1033. https://doi.org/10.1158/2326-6066.CIR-14-0161

Dustin, M.L., Cooper, J.A., 2000. The immunological synapse and the actin cytoskeleton: molecular hardware for T cell signaling. Nat Immunol 1, 23–29. https://doi.org/10.1038/76877

Dustin, M.L., Long, E.O., 2010. Cytotoxic immunological synapses. Immunological Reviews 235, 24–34. https://doi.org/10.1111/j.0105-2896.2010.00904.x

Dynabeads™ Untouched™ Mouse CD8 Cells Kit [WWW Document], n.d. URL https://www.thermofisher.com/order/catalog/product/11417D (accessed 3.26.24).

Finco, T.S., Kadlecek, T., Zhang, W., Samelson, L.E., Weiss, A., 1998. LAT Is Required for TCR-Mediated Activation of PLCγ1 and the Ras Pathway. Immunity 9, 617–626. https://doi.org/10.1016/S1074-7613(00)80659-7

Grakoui, A., Bromley, S.K., Sumen, C., Davis, M.M., Shaw, A.S., Allen, P.M., Dustin, M.L., 1999. The Immunological Synapse: A Molecular Machine Controlling T Cell Activation. Science 285, 221–227. https://doi.org/10.1126/science.285.5425.221

Hanson, D.A., Kaspar, A.A., Poulain, F.R., Krensky, A.M., 1999. Biosynthesis of granulysin, a novel cytolytic molecule. Mol Immunol 36, 413–422. https://doi.org/10.1016/s0161-5890(99)00063-2

Heiniger, H.J., Brunner, K.T., Cerottini, J.C., 1978. Cholesterol is a critical cellular component for T-lymphocyte cytotoxicity. Proceedings of the National Academy of Sciences 75, 5683–5687. https://doi.org/10.1073/pnas.75.11.5683

Henson, J.H., Yeterian, M., Weeks, R.M., Medrano, A.E., Brown, B.L., Geist, H.L., Pais, M.D., Oldenbourg, R., Shuster, C.B., 2015. Arp2/3 complex inhibition radically alters lamellipodial actin architecture, suspended cell shape, and the cell spreading process. Mol Biol Cell 26, 887–900. https://doi.org/10.1091/mbc.E14-07-1244

Hetrick, B., Han, M.S., Helgeson, L.A., Nolen, B.J., 2013. Small Molecules CK-666 and CK-869 Inhibit Actin-Related Protein 2/3 Complex by Blocking an Activating Conformational Change. Chemistry & Biology 20, 701–712. https://doi.org/10.1016/j.chembiol.2013.03.019

Hu, C., Wu, H., Zhu, Q., Cao, N., Wang, H., 2023. Cholesterol metabolism in T-cell aging: Accomplices or victims. The FASEB Journal 37, e23136. https://doi.org/10.1096/fj.202300515R

Huang, J., Brameshuber, M., Zeng, X., Xie, J., Li, Q., Chien, Y., Valitutti, S., Davis, M.M., 2013. A Single Peptide-Major Histocompatibility Complex Ligand Triggers Digital Cytokine Secretion in CD4+ T Cells. Immunity 39, 846–857. https://doi.org/10.1016/j.immuni.2013.08.036

Human CD8+ T Cell Isolation - IN [WWW Document], n.d. URL https://www.thermofisher.com/in/en/home/life-science/cell-analysis/cell-isolation-and-expansion/cell-isolation/human-cell-isolation-products/human-cd8plus-isolation.html (accessed 3.15.24).

Huppa, J.B., Davis, M.M., 2003. T-cell-antigen recognition and the immunological synapse. Nat Rev Immunol 3, 973–983. https://doi.org/10.1038/nri1245

Ikonen, E., 2008. Cellular cholesterol trafficking and compartmentalization. Nat Rev Mol Cell Biol 9, 125–138. https://doi.org/10.1038/nrm2336

Ira Tabas, MD, PhD, Columbia University [WWW Document], n.d. URL https://www.tabaslab.com/protocols/ (accessed 3.14.24).

Koretzky, G.A., Myung, P.S., 2001. Positive and negative regulation of t-cell activation by adaptor proteins. Nat Rev Immunol 1, 95–107. https://doi.org/10.1038/35100523

Korpetinou, A., Skandalis, S.S., Smirlaki, G., Karamanos, N.K., Theocharis, A.D., 2014. Serglycin: At the Crossroad of Inflammation and Malignancy. Front. Oncol. 3. https://doi.org/10.3389/fonc.2013.00327

Kraynov, V.S., Chamberlain, C., Bokoch, G.M., Schwartz, M.A., Slabaugh, S., Hahn, K.M., 2000. Localized Rac Activation Dynamics Visualized in Living Cells. Science 290, 333–337. https://doi.org/10.1126/science.290.5490.333

Krensky, A.M., Clayberger, C., 2009. Biology and clinical relevance of granulysin. Tissue Antigens 73, 193–198. https://doi.org/10.1111/j.1399-0039.2008.01218.x

LI, W., ZHOU, J., XU, Y., 2015. Study of the in vitro cytotoxicity testing of medical devices. Biomed Rep 3, 617–620. https://doi.org/10.3892/br.2015.481

Lippincott-Schwartz, J., Phair, R.D., 2010. Lipids and Cholesterol as Regulators of Traffic in the Endomembrane System. Annual Review of Biophysics 39, 559–578. https://doi.org/10.1146/annurev.biophys.093008.131357

Liu, D., Bryceson, Y.T., Meckel, T., Vasiliver-Shamis, G., Dustin, M.L., Long, E.O., 2009. Integrin-Dependent Organization and Bidirectional Vesicular Traffic at Cytotoxic Immune Synapses. Immunity 31, 99–109. https://doi.org/10.1016/j.immuni.2009.05.009

Lorenzo-Herrero, S., Sordo-Bahamonde, C., Gonzalez, S., López-Soto, A., 2019. CD107a Degranulation Assay to Evaluate Immune Cell Antitumor Activity, in: López-Soto, A., Folgueras, A.R. (Eds.), Cancer Immunosurveillance: Methods and Protocols, Methods in Molecular Biology. Springer, New York, NY, pp. 119–130. https://doi.org/10.1007/978-1-4939-8885-3_7

Lu, F., Liang, Q., Abi-Mosleh, L., Das, A., De Brabander, J.K., Goldstein, J.L., Brown, M.S., 2015. Identification of NPC1 as the target of U18666A, an inhibitor of lysosomal cholesterol export and Ebola infection. eLife 4, e12177. https://doi.org/10.7554/eLife.12177

Ma, X., Bi, E., Lu, Y., Su, P., Huang, C., Liu, L., Wang, Q., Yang, M., Kalady, M.F., Qian, J., Zhang, A., Gupte, A.A., Hamilton, D.J., Zheng, C., Yi, Q., 2019. Cholesterol Induces CD8+ T Cell Exhaustion in the Tumor Microenvironment. Cell Metabolism 30, 143-156.e5. https://doi.org/10.1016/j.cmet.2019.04.002

Ma, Z., Discher, D.E., Finkel, T.H., 2012. Mechanical Force in T Cell Receptor Signal Initiation. Front. Immunol. 3. https://doi.org/10.3389/fimmu.2012.00217

Mahammad, S., Parmryd, I., 2015. Cholesterol Depletion Using Methyl-β-cyclodextrin, in: Owen, D.M. (Ed.), Methods in Membrane Lipids, Methods in Molecular Biology. Springer, New York, NY, pp. 91–102. https://doi.org/10.1007/978-1-4939-1752-5_8

Mahammad, S., Parmryd, I., 2008. Cholesterol homeostasis in T cells. Methyl-β-cyclodextrin treatment results in equal loss of cholesterol from Triton X-100 soluble and insoluble fractions. Biochimica et Biophysica Acta (BBA) - Biomembranes 1778, 1251–1258. https://doi.org/10.1016/j.bbamem.2008.02.010

McCarthy, E.F., 2006. The Toxins of William B. Coley and the Treatment of Bone and Soft-Tissue Sarcomas. Iowa Orthop J 26, 154–158.

Minute, L., Teijeira, A., Sanchez-Paulete, A.R., Ochoa, M.C., Alvarez, M., Otano, I., Etxeberrria, I., Bolaños, E., Azpilikueta, A., Garasa, S., Casares, N., Gracia, J.L.P., Rodriguez-Ruiz, M.E., Berraondo, P., Melero, I., 2020. Cellular cytotoxicity is a form of immunogenic cell death. J Immunother Cancer 8, e000325. https://doi.org/10.1136/jitc-2019-000325

Mok, A.C., Mody, C.H., Li, S.S., 2021. Immune Cell Degranulation in Fungal Host Defence. Journal of Fungi 7, 484. https://doi.org/10.3390/jof7060484

Monks, C.R.F., Freiberg, B.A., Kupfer, H., Sciaky, N., Kupfer, A., 1998. Three-dimensional segregation of supramolecular activation clusters in T cells. Nature 395, 82–86. https://doi.org/10.1038/25764

Mullins, R.D., Heuser, J.A., Pollard, T.D., 1998. The interaction of Arp2/3 complex with actin: Nucleation, high affinity pointed end capping, and formation of branching networks of filaments. Proceedings of the National Academy of Sciences 95, 6181–6186. https://doi.org/10.1073/pnas.95.11.6181

Needham, J., 2000. Science and Civilisation in China, Part 6, Medicine. Cambridge University Press.

Nolte, M.A., ’t Hoen, E.N.M., van Stijn, A., Kraal, G., Mebius, R.E., 2000. Isolation of the intact white pulp. Quantitative and qualitative analysis of the cellular composition of the splenic compartments. European Journal of Immunology 30, 626–634. https://doi.org/10.1002/1521-4141(200002)30:2<626::AID-IMMU626>3.0.CO;2-H

Osińska, I., Popko, K., Demkow, U., 2014. Perforin: an important player in immune response. Cent Eur J Immunol 39, 109–115. https://doi.org/10.5114/ceji.2014.42135

Pathan-Chhatbar, S., Drechsler, C., Richter, K., Morath, A., Wu, W., OuYang, B., Xu, C., Schamel, W.W., 2021. Direct Regulation of the T Cell Antigen Receptor’s Activity by Cholesterol. Front. Cell Dev. Biol. 8. https://doi.org/10.3389/fcell.2020.615996

Poh, M.K., Shui, G., Xie, X., Shi, P.-Y., Wenk, M.R., Gu, F., 2012. U18666A, an intra-cellular cholesterol transport inhibitor, inhibits dengue virus entry and replication. Antiviral Research 93, 191–198. https://doi.org/10.1016/j.antiviral.2011.11.014

Prager, I., Watzl, C., 2019. Mechanisms of natural killer cell-mediated cellular cytotoxicity. Journal of Leukocyte Biology 105, 1319–1329. https://doi.org/10.1002/JLB.MR0718-269R

Radha, G., Lopus, M., 2021. The spontaneous remission of cancer: Current insights and therapeutic significance. Translational Oncology 14, 101166. https://doi.org/10.1016/j.tranon.2021.101166

Ribatti, D., 2016. The concept of immune surveillance against tumors: The first theories. Oncotarget 8, 7175–7180. https://doi.org/10.18632/oncotarget.12739

Riedel, S., 2005. Edward Jenner and the History of Smallpox and Vaccination. Baylor University Medical Center Proceedings 18, 21–25. https://doi.org/10.1080/08998280.2005.11928028

Rizvi, S.A., Neidt, E.M., Cui, J., Feiger, Z., Skau, C.T., Gardel, M.L., Kozmin, S.A., Kovar, D.R., 2009. Identification and Characterization of a Small Molecule Inhibitor of Formin-Mediated Actin Assembly. Chemistry & Biology 16, 1158–1168. https://doi.org/10.1016/j.chembiol.2009.10.006

Rodal, S.K., Skretting, G., Garred, Ø., Vilhardt, F., van Deurs, B., Sandvig, K., 1999. Extraction of Cholesterol with Methyl-β-Cyclodextrin Perturbs Formation of Clathrin-coated Endocytic Vesicles. MBoC 10, 961–974. https://doi.org/10.1091/mbc.10.4.961

Rotty, J.D., Wu, C., Bear, J.E., 2013. New insights into the regulation and cellular functions of the ARP2/3 complex. Nat Rev Mol Cell Biol 14, 7–12. https://doi.org/10.1038/nrm3492

Salata, C., Calistri, A., Parolin, C., Baritussio, A., Palù, G., 2017. Antiviral activity of cationic amphiphilic drugs. Expert Review of Anti-infective Therapy 15, 483–492. https://doi.org/10.1080/14787210.2017.1305888

Sender, R., Weiss, Y., Navon, Y., Milo, I., Azulay, N., Keren, L., Fuchs, S., Ben-Zvi, D., Noor, E., Milo, R., 2023. The total mass, number, and distribution of immune cells in the human body. Proceedings of the National Academy of Sciences 120, e2308511120. https://doi.org/10.1073/pnas.2308511120

Shah, K., Al-Haidari, A., Sun, J., Kazi, J.U., 2021. T cell receptor (TCR) signaling in health and disease. Sig Transduct Target Ther 6, 1–26. https://doi.org/10.1038/s41392-021-00823-w

Shrestha, B., Diamond, M.S., 2007. Fas Ligand Interactions Contribute to CD8+ T-Cell-Mediated Control of West Nile Virus Infection in the Central Nervous System. J Virol 81, 11749–11757. https://doi.org/10.1128/JVI.01136-07

Song, B., 2022. The Cholesterol Transport Inhibitor U18666A Interferes with Pseudorabies Virus Infection. Viruses 14, 1539. https://doi.org/10.3390/v14071539

Stenger, S., Hanson, D.A., Teitelbaum, R., Dewan, P., Niazi, K.R., Froelich, C.J., Ganz, T., Thoma-Uszynski, S., Melián, A., Bogdan, C., Porcelli, S.A., Bloom, B.R., Krensky, A.M., Modlin, R.L., 1998. An Antimicrobial Activity of Cytolytic T Cells Mediated by Granulysin. Science 282, 121–125. https://doi.org/10.1126/science.282.5386.121

Sutton, V.R., Davis, J.E., Cancilla, M., Johnstone, R.W., Ruefli, A.A., Sedelies, K., Browne, K.A., Trapani, J.A., 2000. Initiation of Apoptosis by Granzyme B Requires Direct Cleavage of Bid, but Not Direct Granzyme B–Mediated Caspase Activation. J Exp Med 192, 1403–1414.

Terrén, I., Astarloa-Pando, G., Amarilla-Irusta, A., Borrego, F., 2023. Chapter 3 - P815-based redirected degranulation assay to study human NK cell effector functions, in: Thomas,

C., Galluzzi, L. (Eds.), Methods in Cell Biology, The Immunological Synapse Part A. Academic Press, pp. 33–48. https://doi.org/10.1016/bs.mcb.2022.02.002

Trapani, J.A., 2001. Granzymes: a family of lymphocyte granule serine proteases. Genome Biol 2, reviews3014.1-reviews3014.7.

Ulloth, J.E., Almaguel, F.G., Padilla, A., Bu, L., Liu, J.-W., De Leon, M., 2007. CHARACTERIZATION OF METHYL-β-CYCLODEXTRIN TOXICITY IN NGF-DIFFERENTIATED PC12 CELL DEATH. Neurotoxicology 28, 613–621. https://doi.org/10.1016/j.neuro.2007.01.001

van Gestel, R.A., Helms, J.B., Brouwers, J.F.H.M., Gadella, B.M., 2005. Effects of methyl-beta-cyclodextrin-mediated cholesterol depletion in porcine sperm compared to somatic cells. Mol Reprod Dev 72, 386–395. https://doi.org/10.1002/mrd.20351

Veldkamp, J., Reuver, M.J.D., Willers, J.M.N., 1974. Distribution of different cell types in the lymphoid organs of the mouse, as determined with sera against thymus and Peyer's patches. Immunology 26, 359–366.

Vivier, E., Malissen, B., 2005. Innate and adaptive immunity: specificities and signaling hierarchies revisited. Nat Immunol 6, 17–21. https://doi.org/10.1038/ni1153

Weigelin, B., den Boer, A.T., Wagena, E., Broen, K., Dolstra, H., de Boer, R.J., Figdor, C.G., Textor, J., Friedl, P., 2021. Cytotoxic T cells are able to efficiently eliminate cancer cells by additive cytotoxicity. Nat Commun 12, 5217. https://doi.org/10.1038/s41467-021-25282-3

Yablonski, D., Kuhne, M.R., Kadlecek, T., Weiss, A., 1998. Uncoupling of Nonreceptor Tyrosine Kinases from PLC-γ1 in an SLP-76-Deficient T Cell. Science 281, 413–416. https://doi.org/10.1126/science.281.5375.413

Yan, C., Zheng, L., Jiang, S., Yang, H., Guo, J., Jiang, L., Li, T., Zhang, H., Bai, Y., Lou, Y., Zhang, Q., Liang, T., Schamel, W., Wang, H., Yang, W., Wang, G., Zhu, Z., Song,

B.-L., Xu, C., 2023. Exhaustion-associated cholesterol deficiency dampens the cytotoxic arm of antitumor immunity. Cancer Cell 0. https://doi.org/10.1016/j.ccell.2023.04.016

Yang, S.-T., Kreutzberger, A.J.B., Lee, J., Kiessling, V., Tamm, L.K., 2016. The role of cholesterol in membrane fusion. Chemistry and Physics of Lipids, Properties and Functions of Cholesterol 199, 136–143. https://doi.org/10.1016/j.chemphyslip.2016.05.003

Yang, W., Bai, Y., Xiong, Y., Zhang, J., Chen, S., Zheng, X., Meng, X., Li, L., Wang, J., Xu, Chenguang, Yan, C., Wang, L., Chang, C.C.Y., Chang, T.-Y., Zhang, T., Zhou, P., Song, B.-L., Liu, W., Sun, S., Liu, X., Li, B., Xu, Chenqi, 2016. Potentiating the antitumour response of CD8+ T cells by modulating cholesterol metabolism. Nature 531, 651–655. https://doi.org/10.1038/nature17412

Yeagle, P.L., 2022. Unraveling a mystery: Why human cells require cholesterol. Science Advances 8, eade5927. https://doi.org/10.1126/sciadv.ade5927

Żal, T., Żal, M.A., Gascoigne, N.R.J., 2002. Inhibition of T Cell Receptor-Coreceptor Interactions by Antagonist Ligands Visualized by Live FRET Imaging of the T-Hybridoma Immunological Synapse. Immunity 16, 521–534. https://doi.org/10.1016/S1074-7613(02)00301-1

Zhang, H., Yu, X., Ye, J., Li, H., Hu, J., Tan, Y., Fang, Y., Akbay, E., Yu, F., Weng, C., Sankaran, V.G., Bachoo, R.M., Maher, E., Minna, J., Zhang, A., Li, B., 2023. Systematic investigation of mitochondrial transfer between cancer cells and T cells at single-cell resolution. Cancer Cell 41, 1788-1802.e10. https://doi.org/10.1016/j.ccell.2023.09.003

Zidovetzki, R., Levitan, I., 2007. Use of cyclodextrins to manipulate plasma membrane cholesterol content: Evidence, misconceptions and control strategies. Biochimica et

Biophysica Acta (BBA) - Biomembranes 1768, 1311–1324.

https://doi.org/10.1016/j.bbamem.2007.03.026